Arctic Ocean during the Last Glacial Maximum: Atlantic and polar domains of surface water mass distribution and ice cover

Niels Nørgaard-Pedersen,[1,2] Robert F. Spielhagen,[2] Helmut Erlenkeuser,[3] Pieter M. Grootes,[3] Jan Heinemeier,[4] and Jochen Knies[5]

[1] On the basis of 52 sediment cores, analyzed and dated at high resolution, the paleoceanography and climate of the Last Glacial Maximum (LGM) were reconstructed in detail for the Fram Strait and the eastern and central Arctic Ocean. Sediment composition and stable isotope data suggest three distinct paleoenvironments: (1) a productive region in the eastern to central Fram Strait and along the northern Barents Sea continental margin characterized by Atlantic Water advection, frequent open water conditions, and occasional local meltwater supply and iceberg calving from the Barents Sea Ice Sheet; (2) an intermediate region in the southwestern Eurasian Basin (up to 84–85°N) and the western Fram Strait characterized by subsurface Atlantic Water advection and recirculation, a moderately high planktic productivity, and a perennial ice cover that breaks up only occasionally; and (3) a central Arctic region (north of 85°N in the Eurasian Basin) characterized by a low-salinity surface water layer and a thick ice cover that strongly reduces bioproduction and bulk sedimentation rates. Although the total inflow of Atlantic Water into the Arctic Ocean may have been reduced during the LGM, its impact on ice coverage and halocline structure in the Fram Strait and southwestern Eurasian Basin was strong.   *INDEX TERMS:* 4267 Oceanography: General: Paleoceanography; 9315 Information Related to Geographic Region: Arctic region; 1620 Global Change: Climate dynamics (3309); 1635 Global Change: Oceans (4203); *KEYWORDS:* Arctic Ocean, Last Glacial Maximum, Atlantic Water advection, planktic foraminifers, oxygen isotopes, sea ice

1. Introduction

[2] This paper arose from a joint German research program on Last Glacial Maximum (LGM) conditions in the Atlantic (GLAMAP 2000) [*Sarnthein et al.*, 2003a]. The main objective of the program was to reconstruct up-to-date sea surface temperature (SST) maps of the entire Atlantic Ocean for the LGM period as boundary conditions and control for 3-D global circulation models. LGM objectives of particular interest for the high northern latitudes are to assess variations in sea ice cover, the intensity of past deep-water formation in the North Atlantic, and the amount of cross-equatorial heat advection from the central and southern Atlantic into the Norwegian, Greenland, and Iceland seas (the "Nordic Seas").

[3] Here we focus on LGM paleoceanographic conditions in the Arctic Ocean and the Fram Strait connection to the Nordic Seas and the Atlantic realm. While the reconstruction of SSTs from planktic foraminifer associations was performed by GLAMAP 2000 partners [*Pflaumann et al.*, 2003], we have used oxygen and carbon isotope records of *Neogloboquadrina pachyderma* (s) and abundance/flux records of planktic foraminifers and ice-rafted debris (IRD) in order to reconstruct the position of oceanographic fronts and the summer sea ice margin. Using data sets from 26 analyzed sediment cores and from published sources (other 26 cores), we were also able to reconstruct the character of the ice cover and deduce circulation patterns of the main surface water masses in the area.

[4] During the LGM, environmental boundary conditions in the Arctic were profoundly different from the present interglacial. Sea level was lowered and the huge Arctic shelf areas were either exposed or covered by ice sheets [*Svendsen et al.*, 1999; *Zreda et al.*, 1999; *Dyke et al.*, 2002]. Consequently, important gateways for the exchange of water masses with the world ocean were closed, except the >2500 m deep Fram Strait connection to the Nordic Seas. A huge ice sheet was centered over the Barents Sea [*Elverhøi and Solheim*, 1983; *Svendsen et al.*, 1999] blocking Atlantic Water supply to the Arctic Ocean through this presently important branch. Most parts of the Canadian

_____

[1]School of Geography and Geosciences, University of St. Andrews, Scotland, UK.
[2]Research Center for Marine Geosciences, GEOMAR, Kiel University, Kiel, Germany.
[3]Leibniz Laboratory, Kiel University, Kiel, Germany.
[4]Accelerator Mass Spectrometry [14]C Dating Laboratory, Institute of Physics and Astronomy, University of Aarhus, Aarhus, Denmark.
[5]Geological Survey of Norway, Trondheim, Norway.

archipelago were covered by the northern Laurentide Ice Sheet [*Dyke et al.*, 2002]. The Innuitian Ice Sheet over Ellesmere Island coalesced with the Greenland Ice Sheet and blocked the Nares Strait connection to the Baffin Bay and Labrador Sea [*England*, 1999; *Zreda et al.*, 1999]. The shallow Bering Strait connection to the Pacific and the huge Siberian shelves were subaerially exposed and covered by a periglacial tundra steppe [*Hopkins*, 1982; *Sher*, 1995; *Elias et al.*, 1996]. Model simulations of the LGM climate show that the expansion of ice sheets over North America and NW Eurasia caused severe changes in atmospheric temperatures, pressure gradients, and geostrophic wind patterns [*Kutzbach and Guetter*, 1986; *Ganopolski et al.*, 1998; *Kageyama et al.*, 2001], which must also have influenced the Arctic Ocean environment. Paleobotanical data [*Tarasov et al.*, 1999] support model outputs, which indicate a much drier and colder climate in the ice sheet-free areas of northern Eurasia than today, resulting in a decreased freshwater supply from Siberian rivers. On the other hand, release of icebergs and subsequent melting may in some regions have been an important freshwater source [*Stein et al.*, 1994]. The total amount of Atlantic Water supplied to the Nordic Seas and the Arctic Ocean was reduced during the LGM [*Seidov and Haupt*, 1997; *Kuijpers et al.*, 1998; *Chapman and Maslin*, 1999].

[5] Based on the distribution of planktic microfossils and IRD, the *CLIMAP Project Members* [1976, 1981] Working Group concluded that the Nordic Seas were perennially ice-covered during the LGM. Their results placed the polar front and winter ice margin zonally across the North Atlantic from west to east as far south as 45°N. *Hebbeln et al.* [1994] presented the first evidence for a meridional circulation pattern and showed that seasonally ice-free waters were present during most of the LGM in the Norwegian Sea up to Svalbard. Based on the regional distribution of planktic foraminiferal stable isotope data and transfer function SST estimates, subsequent studies [e.g., *Sarnthein et al.*, 1995, 2003b; *Weinelt et al.*, 1996] also concluded that great parts of the Nordic Seas were ice free during LGM summers. Analyses of dinocyst assemblages [*de Vernal et al.*, 2000] and alkenone proxy data (U_{37}^k) [*Rosell-Melé and Koç*, 1997] suggest unexpectedly high summer SST estimates for the LGM in the Nordic Seas. The authors, however, state that these results should be considered with caution because they may be biased by low bioproductivity and sedimentation rates as well as the possible input of allochthonous material [cf. *Rosell-Melé and Comes*, 1999; *de Vernal et al.*, 2000]. *Knies et al.* [1999] found enhanced total organic carbon (TOC) accumulation rates and high contents of biogenic carbonate (nannoplankton and calcareous foraminifers) in the LGM interval in sediment cores from the northern Barents Sea continental margin, suggesting the penetration of Atlantic surface water into the Arctic Ocean along the margin of the Barents Sea Ice Sheet. They proposed that a major flaw lead (polynya) formed, with at least seasonally open waters and a relatively high bioproduction, due to katabatic winds blowing off the ice sheet. On the other hand, sediment cores from the central Arctic Ocean and the Amerasian Basin [*Darby et al.*, 1997; *Nørgaard-Pedersen et al.*, 1998; *Poore et al.*,

1999] reveal that marine oxygen isotope stage (MIS) 2 (including the LGM) in these areas was a period of very limited bioproduction and extremely low sedimentation rates, resulting from massive sea ice cover with limited seasonal variation. The distribution of ^{14}C ages in some cores from the western Arctic Ocean [*Darby et al.*, 1997; *Poore et al.*, 1999] suggests a nondepositional hiatus during the LGM, therefore, the possibility of an ice shelf floating over that part of the Arctic Ocean cannot be ruled out. Two decades ago, *Hughes et al.* [1977] and *Denton and Hughes* [1981] put forward the hypothesis of a floating thick ice sheet over the Arctic Ocean connected to circum-Arctic continental ice sheets. According to these authors, the calving ice margin of a LGM Arctic ice sheet was situated south of the Iceland-Faroe Ridge. Since then, in situ data from many parts of the Arctic Ocean and its margins have shown that the idea of one giant Northern Hemisphere ice sheet during the LGM is not well substantiated and that the extension of LGM ice sheets in northern Eurasia was much smaller than supposed by the *CLIMAP Project Members* [1981] Working Group [cf. *Hopkins*, 1982, *Markussen et al.*, 1985; *Sher*, 1995; *Velichko et al.*, 1997; *Velichko*, 1995; *Nørgaard-Pedersen et al.*, 1998; *Svendsen et al.*, 1999, *Mangerud et al.*, 2002]. Despite this wealth of field data, the idea of a huge LGM ice sheet covering the entire northern Eurasian continental margin is still supported by some authors [e.g., *Grosswald and Hughes*, 2002].

2. Modern Interglacial Conditions

[6] Today the Arctic Ocean, perennially covered by sea ice, is a semienclosed well-stratified sea, with the Fram Strait and the Barents Sea as major conduits exchanging Atlantic Water and low-salinity polar surface water and sea ice (Figure 1). Import of Pacific Water through the shallow Bering Strait and export of water masses via the Canadian archipelago are also important for the Arctic Ocean halocline characteristics and nutrient supply [*Anderson et al.*, 1994]. Although the deep Arctic Ocean experiences more severe winter conditions than the Greenland Sea, no deep convection takes place due to the low salinity surface layer, which is fed by the huge freshwater discharge from circum-Arctic rivers ($\sim 3 \times 10^6$ km^3/year) [*Aagaard and Carmack*, 1989], effectively forming a lid over the layer of warmer (0–2°C) and more saline Atlantic Water. Fundamentally, this is why the Arctic Ocean is perennially sea ice covered [*Aagaard and Carmack*, 1994].

[7] The extent of sea ice cover in the Fram Strait reflects the interaction between Atlantic Water and polar water masses. On the western side of the Fram Strait, the East Greenland Current (EGC) carries cold polar water (about −1.5°C; salinity about 32) and sea ice southward. In the eastern Fram Strait, Atlantic Water in the West Spitsbergen Current (WSC), with maximum SSTs of about 5°C and high salinities (about 35), maintains year-round ice-free conditions. Entering the Arctic Ocean, the Atlantic Water submerges beneath the polar low salinity surface layer and continues as a boundary current eastward along the northern Barents Sea margin [*Rudels et al.*, 1994]. Mesoscale eddies generated on the western edge of the WSC also carry
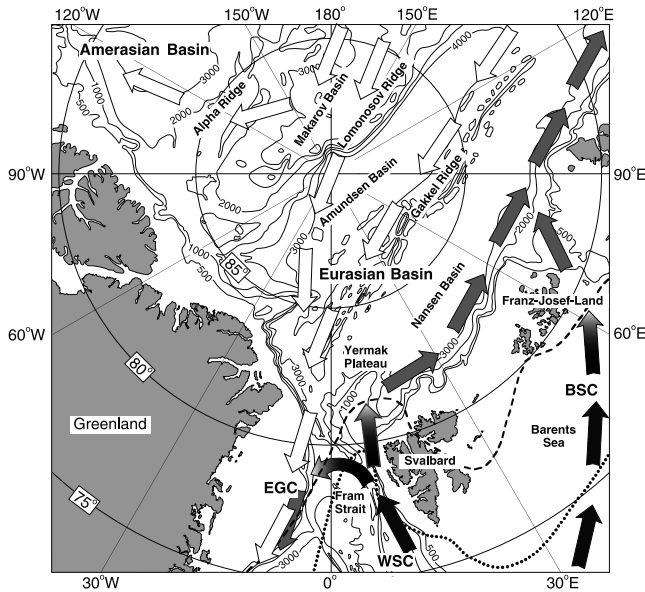
Figure 1. Bathymetry and distribution of modern surface-subsurface currents in the Arctic Ocean-Fram Strait region. Black arrows denote Atlantic surface water advected northward. Hatched arrows represent submerged Atlantic Water continuing along the Eurasian continental margin as a boundary current. White arrows denote the circulation pattern of low salinity polar surface water. The mean positions of the sea ice margin during summer (dashed line) and winter (dotted line) are shown. Abbreviations are as follows: WSC, West Spitsbergen Current; EGC, East Greenland Current; and BSC, Barents Sea Current.

Atlantic Water westward across the Fram Strait, where it submerges beneath the EGC and flows southward again as the subsurface Return Atlantic Current [*Bourke et al.*, 1988].

[8] Present-day ice cover in the Fram Strait (Figure 1) is highly variable, with permanently and seasonally ice-free areas [*Vinje*, 1977, 1985]. The summer ice margin can move up to 200–300 km north of Svalbard. Seasonal changes in temperature and wind patterns cause the ice cover to expand considerably during winter. From observations over the past decades it has been suggested that the variable locations of oceanic fronts, the thickness of the Arctic halocline and the sea ice cover are all subject to decadal-scale oscillations [*Morison et al.*, 1998; *Dickson*, 1999; *Rothrock et al.*, 1999]. The duration and degree of sea ice cover significantly influences lithogenic and biogenic particle fluxes and sedimentation rates [*Hebbeln and Wefer*, 1991; *Carstens et al.*, 1997]. Under a complete, perennial ice cover, which limits the penetration of light, fluxes of both particle types are very low. While maximum biogenic fluxes occur in (seasonally) open waters, the marginal ice zone defines the area of highest lithogenic sedimentation rates, released from melting sea ice [*Hebbeln*, 2000]. The absolute abundances of planktic foraminifers in the upper water column show a similar spatial pattern. Under a perennial ice cover, abundances are about a factor of 10 lower than in open water and ice-marginal regions [*Carstens and Wefer*, 1992; *Volkmann*,

2000]. Moreover, the preferred habitat depth of Arctic polar and subpolar planktic foraminifers is about 100–300 m in open water and ice-marginal settings (i.e., in the upper Atlantic Water layer). In the perennially ice-covered interior of the Arctic Ocean, planktic foraminifers are forced, due to limited food availability and reduced light penetration, to dwell in the low salinity and cold polar water that characterize the upper 100 m [*Carstens and Wefer*, 1992; *Carstens et al.*, 1997; *Volkmann*, 2000]. This habitat change is important when interpreting isotope records and summer SST estimates.

3. Strategy and Methods

[9] The high-resolution stratigraphic framework for the LGM in the 52 sediment cores used for this study (Table 1, Figure 2) is based on accelerator mass spectrometry (AMS) ^{14}C dates available for 32 of these cores. The other cores were correlated to the dated cores using stable isotope records and sedimentological parameters described below. Sources for published data are given in Table 1; additional AMS ^{14}C dates are listed in Table 2. AMS ^{14}C dates were obtained on monospecific planktic foraminifer samples (10–20 mg of *N. pachyderma* (s)) with the exception of two samples in which benthic foraminifers were dated. The ^{14}C measurements were performed at the Leibniz Laboratory of Kiel University and the Institute for Physics and Astronomy of Aarhus University. All ^{14}C dates were corrected for a marine radiocarbon reservoir effect equal to 400 years. It should be noted, however, that the ^{14}C reservoir effect of seawater is likely to have been considerably larger and variable during periods of MIS 2 and 3 [*Voelker et al.*, 1998]. In addition to this temporal variation in reservoir effect, a geographic variability may exist between regions influenced by North Atlantic and Arctic water masses [e.g., *Haflidason et al.*, 2000; *Eiriksson et al.*, 2000], although the magnitude of such an effect during the LGM in the Arctic Ocean proper remains unknown. Radiocarbon ages were converted to calendar ages (cal. ka) with the CALIB 4.3 calibration program [*Stuiver and Reimer*, 1993; *Stuiver et al.*, 1998] and, beyond 20.3 ^{14}C ka, by applying the age calibration determined by *Voelker et al.* [1998]. Age determinations between dated levels were based on linear interpolation assuming constant sedimentation rates between fixed points.

[10] The GLAMAP 2000 LGM time slice used in this study comprises the time interval 15–18 ^{14}C ka (~18.0–21.5 cal. ka), which in oxygen isotope records from the Nordic Seas is known to be a period of climatic stability and minimum meltwater influx [*Sarnthein et al.*, 1995]. Since in some southern Atlantic records deglacial warming is already recorded in the younger part of the GLAMAP 2000 LGM time slice, the EPILOG working group [*Mix et al.*, 2001] suggested a definition of the LGM (LGM Chronozone Level 2 of *Mix et al.* [2001]: 16.0–19.5 ^{14}C ka or 19.0–23.0 cal. ka) slightly different from the GLAMAP 2000 LGM time slice. Oxygen isotope (δ^{18}O) values of the planktic foraminifer *N. pachyderma* (s) in the size range 125–250 μm from Arctic Ocean surface sediments generally show a good correlation to the surface water salinity [*Spielhagen and Erlenkeuser*, 1994]. Today, highest

Table 1. List of Sediment Cores Used For This Study, Including Depth of the LGM Interval and GLAMAP 2000 LGM Oxygen Isotope Data

Core	Latitude	Longitude	Water Depth, m	LGM Depth Interval, cm	$\delta^{13}O$, Average, ‰ PDB	$\delta^{18}O$ Maximum, ‰ PDB	$\delta^{18}O$ Minimum, ‰ PDB	Source
FRAM I/4	84°29.9′N	08°58.7′W	3820	15–23	4.59	4.70	4.46	*Markussen et al.* [1985]
FRAM I/7	83°52.6′N	06°57.3′W	2990	26–40	4.61	4.69	4.56	*Markussen et al.* [1985]
M17725-1	77°27.6′N	4°34.7′E	2577	25–40	4.31	4.42	4.13	*Weinelt et al.* [1996]
NP90-12	78°24.5′N	09°24.9′E	628	220–275	4.65	4.75	4.55	*Dokken* [1995]
NP90-36	77°37.0′N	09°56.2′E	1360	330–360	4.60	4.70	4.30	*Dokken* [1995]
NP90-39	77°15.5′N	09°05.6′E	2119	127–155	4.48	4.72	4.30	*Dokken* [1995]
OD-009-11	86°22.9′N	144°20.4′E	995	17–18	2.67	–	–	own data
OD-010-04	86°23.9′N	142°56.9′E	1007	20–21	2.56	–	–	own data
OD-031-03	85°39.5′N	160°35.0′E	3586	15–16	2.20	–	–	own data
OD-036-04	89°00.0′N	179°55.4′E	2271	8–9	2.22	–	–	own data
OD-041-04	84°01.8′N	11°14.30′E	3344	13–17	4.76	4.81	4.70	own data
PS1230-1	78°51.5′N	04°46.5′W	2700	20–28	4.28	4.74	3.69	own data
PS1294-4	77°59.9′N	05°22.3′E	2668	35–55	4.75	4.80	4.70	*Hebbeln and Wefer* [1997]
PS1295-4	77°59.2′N	02°24.8′E	3112	36–43	4.63	4.71	4.52	*Jones and Keigwin* [1988]
PS1297-4/3	78°00.8′N	01°00.8′W	3051	18–30	4.65	4.70	4.60	*Hebbeln and Wefer* [1997]
PS1308-3	80°01.0′N	04°49.8′W	1444	20–32	3.95	4.25	3.80	own data
PS1314-3	80°00.1′N	04°29.7′E	1382	21–28	4.22	4.46	4.04	own data
PS1524-1	85°21.5′N	26°19.9′E	3634	13–15	3.65	3.70	3.60	*Köhler* [1992]
PS1527-10	86°05.8′N	22°01.0′E	3704	10–12	3.93	4.00	3.85	*Köhler* [1992]
PS1528-7	86°07.8′N	23°09.5′E	3972	10–12	3.95	4.00	3.90	*Köhler* [1992]
PS1533-3	82°01.9′N	15°10.7′E	2030	60–85	4.60	4.67	4.53	*Köhler* [1992]
PS1535-5/8	78°45.1′N	01°51.0′E	2557	32–47	4.74	4.81	4.70	own data
PS1894-9	75°48.8′N	08°18.0′W	1975	36–125	4.39	4.61	3.91	own data
PS1906-1	76°55.5′N	02°09.0′W	2990	21–30	4.25	4.70	3.02	own data
PS2122-2	80°23.4′N	07°33.0′E	705	159–200	4.20	4.41	3.60	*Knies* [1994]
PS2123-2	80°10.4′N	09°51.4′E	571	187–228	4.43	4.59	4.34	*Knies* [1994]
PS2129-1	81°22.0′N	17°28.3′E	861	20–40	4.68	4.73	4.60	*Knies* [1999]
PS2138-1	81°32.1′N	30°35.6′E	995	130–215	4.44	4.58	4.29	*Knies et al.* [1999]
PS2163-1	86°14.5′N	59°12.9′E	3040	10–11	3.50	–	–	*Stein et al.* [1994]
PS2166-2	86°51.6′N	59°45.9′E	3636	18–19	3.68	–	–	*Nørgaard-Pedersen* [1997]
PS2170-4	87°35.8′N	60°53.7′E	4083	14–16	3.50	–	–	*Stein et al.* [1994]
PS2172-5	87°15.4′N	68°22.7′E	4391	18–19	3.54	–	–	*Nørgaard-Pedersen* [1997]
PS2177-1	88°02.2′N	134°55.1′E	1388	17–18	2.42	–	–	*Nørgaard-Pedersen* [1997]
PS2178-2	88°00.2′N	159°14.0′E	4009	11–12	2.09	–	–	*Nørgaard-Pedersen* [1997]
PS2179-1	87°44.8′N	138°01.7′E	1230	17–18	2.92	–	–	*Nørgaard-Pedersen* [1997]
PS2180-1	87°37.6′N	156°40.5′E	4005	9–10	1.67	–	–	*Nørgaard-Pedersen* [1997]
PS2185-3	87°31.9′N	144°22.9′E	1051	12–13	2.89	–	–	*Nørgaard-Pedersen* [1997]
PS2186-5	88°30.9′N	140°29.4′E	2036	16–17	2.51	–	–	*Nørgaard-Pedersen* [1997]
PS2193-2	87°31.1′N	11°15.5′E	4337	13–14	3.44	–	–	*Nørgaard-Pedersen* [1997]
PS2195-4	86°13.7′N	09°35.6′E	3873	9–10	4.02	–	–	*Nørgaard-Pedersen* [1997]
PS2196-2	85°57.1′N	00°06.9′E	3958	9–10	3.77	–	–	*Nørgaard-Pedersen* [1997]
PS2200-2	85°19.6′N	14°00.0′W	1074	6–7	4.22	–	–	*Nørgaard-Pedersen* [1997]
PS2206-4	84°16.7′N	02°30.3′W	2993	10–13	4.60	–	–	*Stein et al.* [1994]
PS2208-1	83°38.4′N	04°36.2′E	3681	15–25	4.60	4.80	4.50	*Stein et al.* [1994]
PS2210-3	83°02.3′N	10°04.0′E	3702	12–14	4.65	–	–	*Stein et al.* [1994]
PS2212-3	82°04.2′N	15°51.2′E	2550	80–100	4.26	4.27	4.25	*Vogt* [1997]
PS2423-4	80°02.3′N	05°26.9′W	829	20–100	3.80	4.10	3.30	*Notholt* [1998]
PS2424-1	80°02.1′N	05°44.6′W	445	390–433	4.20	4.40	4.00	*Notholt* [1998]
PS2446-4	82°23.8′N	40°54.5′E	2022	180–210; 300–340	4.30	4.50	4.20	*Knies et al.* [1999]
PS2837-5	81°14.0′N	02°24.7′E	1023	389–397	4.72	4.81	4.61	own data
PS2876-1/2	81°45.7′N	09°24.0′W	1991	9–62	4.55	4.95	4.28	own data
PS2887-1	79°36.0′N	04°36.5′W	1411	52–35	3.33	4.62	2.20	own data

$\delta^{18}O$ values come from areas influenced by the inflow of saline Atlantic Water, whereas values of specimens, which have lived in the low-salinity polar surface water layer, are up to 2.5‰ lower. However, derivation of paleosalinities in stratified waters is complicated by the fact that planktic foraminifers undergo secondary gametogenic calcification in deeper waters during their final life stage [*Kohfeld et al.*, 1996; *Bauch et al.*, 1997]. Moreover, along oceanographic fronts, where water masses converge and subducting below each other, attempts to reconstruct surface ocean conditions are problematic. Despite these limitations, the spatial dis-

tribution of $\delta^{18}O$ values was used to reconstruct the distribution of Atlantic and polar water masses in the LGM time slices. Flux records of planktic foraminifers served as a relative productivity proxy reflecting nutrient supply and light penetration coupled to the degree of ice cover [*Hebbeln and Wefer*, 1991]. The ice-rafted debris (IRD) content was used to roughly estimate the input of terrigenous sediments transported by icebergs derived from continental ice sheets calving into the Arctic Ocean.

[11] From the analyzed cores, 30–50 cm³ samples were obtained as 1–2 cm thick sediment slices at intervals of
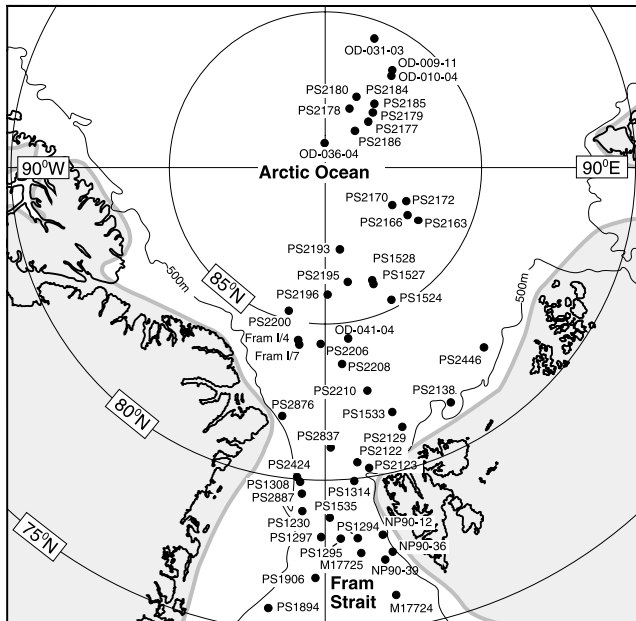
Figure 2. Location of sediment cores used from the Fram Strait and the adjacent Arctic Ocean (listed in Table 1). The approximate extension of continental ice sheets during the LGM is indicated.

1–5 cm depending on stratigraphic resolution. After freeze-drying, the samples were washed through a 63 μm mesh with deionized water. After drying, the >63 μm fraction was sifted with a sonic sifter into 5 subfractions (63–125 μm, 125–250 μm, 250–500 μm, 500–1000 μm, >1000 μm). Fixed-volume samples (10 cm^3) for determination of wet and dry bulk density were taken at intervals of 5–10 cm and dry bulk density values of samples in between were interpolated. Bulk accumulation rates (BAR; g cm^{-2} kyr^{-1}) were determined following *Ehrmann and Thiede* [1985]. Stable oxygen (δ^{18}O) and carbon (δ^{13}C) isotope values were measured on ∼25 specimens of equally sized, four-chambered *N. pachyderma* (s) from the 125–250 μm fraction. The measurements were carried out at the Leibniz Laboratory, University of Kiel, on a Finnigan MAT 251 mass spectrometer, equipped with the automated Carbo-Kiel carbonate device. The δ^{18}O and δ^{13}C values were calibrated to the PDB scale using the standard National Bureau of Standards (NBS) 20 calcite and have an analytical precision of 0.07‰ for δ^{18}O and 0.04‰ for δ^{13}C.

[12] Abundances of planktic foraminifers (125–250 μm) per gram dry sediment and possible carbonate dissolution effects were determined microscopically on representative sample splits using ∼400 grains. Where planktic foraminifers were rare, sample splits of >1000 grains were used. The flux of planktic foraminifers (specimens cm^{-2} kyr^{-1}) was calculated as the product of BAR and the absolute abundance of planktic foraminifers (specimens g^{-1}) in the respective sample. The grain-size fraction >500 μm (wt %) was used as a proxy for the abundance of coarse IRD. Sea ice may also transport sandy material, but usually the rafted material is dominated by silt and clay [*Nürnberg et al.*,

1994]. To avoid "contamination" from other sources such as sea ice, only particles >500 μm were considered [cf. *Clark and Hanson*, 1983; *Spielhagen*, 1991; *Hebbeln*, 2000]. In none of the analyzed LGM samples did this fraction contain significant amounts of biogenic grains. Data sets of previously unpublished records are available from the German paleoclimate data repository PANGAEA: http://www. pangaea.de.

4. Results

4.1. Sedimentation Rates and Stratigraphic Resolution

[13] The radiocarbon dates (Table 2) and the oxygen isotope records are the basis for the stratigraphic delimitation of the LGM interval. Sedimentation rates and stratigraphic resolution vary strongly depending on core location (Figure 3). Highest sedimentation rates in the LGM interval (25–50 cm kyr^{-1}) are found at the continental slope sites off the northern Barents Sea (PS2138) and off NE Greenland (PS2876). Both sites are situated close to the LGM continental ice sheet margins [*Landvik et al.*, 1998; *Svendsen et al.*, 1999; *Funder and Hansen*, 1996]. In the Fram Strait and the Yermak Plateau records, LGM sedimentation rates are in the range of 2–10 cm kyr^{-1} and tend to decrease toward the west. Hemipelagic sedimentation rates in the southwestern Eurasian Basin (selected turbidite-protected sites) are limited to ca. 1–3 cm kyr^{-1}. Away from the continental margins, between 84°N and 85°N, further reductions in LGM sedimentation rates are observed. This trend continues northward, so that north of 85°N, hemipelagic sedimentation rates are only a few mm kyr^{-1} through MIS 2.

4.2. Stable Isotope Data

[14] The analyzed oxygen isotope records (Figures 4 and 5) generally show highest values in MIS 2 and values 1–2‰ lower in the post-glacial interval. Decreasing δ^{18}O values in the late stage of the LGM interval were recorded in the central Fram Strait-Yermak Plateau-Northern Barents Sea region at about 18.5–16 cal. ka. This probably reflects an abrupt lowering of regional surface water salinities related to the discharge of isotopically light meltwater during the early deglaciation of the Barents Sea Ice Sheet [cf. *Jones and Keigwin*, 1988; *Elverhøi et al.*, 1995] and possibly the Arctic Laurentide/Innuitian Ice Sheets [*Darby et al.*, 2002]. Reduced δ^{13}C values during such events, caused by a decreased ventilation/increased stratification of the surface water masses [*Sarnthein et al.*, 1995], support this interpretation. *Jones and Keigwin* [1988] and *Elverhøi et al.* [1995] reported ages of about 15–14 ^{14}C ka (17.8–16.7 cal. ka) for the early deglaciation in the Fram Strait region.

[15] Between 76°N and 80°N along the Northeast Greenland continental margin (sites PS2887, PS1230, PS1906), high LGM δ^{18}O values were found only in the period 22.5–20.5 cal. ka. This interval is terminated by a prominent low-δ^{18}O event lasting from about 20.5 to 18.5 cal. ka. Due to the proximity of these sites to the expanded Greenland ice sheet during the LGM, this event may have been caused by a regional meltwater event. However, it is also possible that these sites may have been influenced by a subsurface water

Table 2. Results of Accelerator Mass Spectrometer [14]C Dates Performed for This Study

| Core	Depth, cm	Species Dated	[14]C Age,[a] [14]C years BP	Error, ± years	Cal. Age,[b] years BP	Laboratory
PS1894-7	0.5	*N. pachyderma (s.)*	3845	40	3810	KIA7088
PS1894-7	9.5	*N. pachyderma (s.)*	5745	40	6170	KIA7089
PS1894-7	21.5	*N. pachyderma (s.)*	8910	55	9460	KIA7090
PS1894-7	35.5	*N. pachyderma (s.)*	14430	70	16710	KIA7091
PS1894-9	1 (43)	*N. pachyderma (s.)*	17350	40	20530	KIA7085
PS1894-9	81 (123)	*N. pachyderma (s.)*	17110	40	20250	KIA7086
PS1894-9	91 (133)	*N. pachyderma (s.)*	18600	55	21970	KIA7087
PS1906-1	4.5	*N. pachyderma (s.)*	3960	30	4500	KIA7084
PS1906-1	11.5	*N. pachyderma (s.)*	7565	40	8400	KIA7083
PS1906-1	22.5	*N. pachyderma (s.)*	16640	80	19710	KIA7082
PS1906-1	32.5	*N. pachyderma (s.)*	18730	90	22120	KIA7081
PS1906-2	35 (21.9)	*N. pachyderma (s.)*	16520	80	19570	KIA7078
PS1906-2	46 (31)	*N. pachyderma (s.)*	18380	90	21715	KIA7079
PS1906-2	103 (88.5)	*N. pachyderma (s.)*	27440	220	31900	KIA7080
PS1533-3	68	*N. pachyderma (s.)*	16250	120/110	19260	KIA4170
PS1535-5	0	mixed benthic foram.	240	20	282	KIA4171
PS1535-5	7.5	*N. pachyderma (s.)*	4970	40	5720	KIA1468
PS1535-8	35	*N. pachyderma (s.)*	16250	170	19260	AAR-1788
PS1535-8	45	*N. pachyderma (s.)*	17750	250	21020	AAR-1787
PS1535-8	75	*N. pachyderma (s.)*	24150	300	28150	AAR-1789
PS1535-8	89	*N. pachyderma (s.)*	29400	280	33250	AAR-3078
PS1535-8	97	*N. pachyderma (s.)*	31500	260	35150	AAR-3079
PS1535-8	109	*N. pachyderma (s.)*	33050	450	36700	AAR-3080
PS2837-6	10.5	*N. pachyderma (s.)*	135	25	140	KIA7570
PS2837-5	50.5	*N. pachyderma (s.)*	1730	40	1700	KIA4652
PS2837-5	76.5	*N. pachyderma (s.)*	2940	35	3202	KIA8927
PS2837-5	111.5	*N. pachyderma (s.)*	4565	45	5300	KIA8928
PS2837-5	153.5	*N. pachyderma (s.)*	7005	45	7850	KIA8929
PS2837-5	182.5	*N. pachyderma (s.)*	7670	60	8530	KIA4653
PS2837-5	225.5	*N. pachyderma (s.)*	8890	60	9850	KIA8930
PS2837-5	253.5	*N. pachyderma (s.)*	10540	50	12460	KIA7571
PS2837-5	274.5	*N. pachyderma (s.)*	11755	60	13630	KIA10863
PS2837-5	300.5	*N. pachyderma (s.)*	12255	60	14310	KIA7572
PS2837-5	359.5	*N. pachyderma (s.)*	12540	70	14360	KIA10864
PS2837-5	382.5	*N. pachyderma (s.)*	15640	80	18560	KIA10865
PS2837-5	389.5	*N. pachyderma (s.)*	17040	110	20160	KIA4654
PS2837-5	415.5	*N. pachyderma (s.)*	23830	180	27750	KIA7573
PS2837-5	497.5	*N. pachyderma (s.)*	48760	4810/2990	50050	KIA4655
PS2876-1	0	*N. pachyderma (s.)*	6390	70	7260	KIA6123
PS2876-1	6.5	*N. pachyderma (s.)*	7820	45	8650	KIA6124
PS2876-1	9.5	*N. pachyderma (s.)*	14110	90/80	16920	KIA6125
PS2876-1	17.5	*N. pachyderma (s.)*	16450	90	19490	KIA6126
PS2876-1	17.5	*N. pachyderma (s.)*	16600	90	19670	KIA6126
PS2876-2	62	*N. pachyderma (s.)*	17950	150	21420	KIA6127
PS2876-2	87.5	*N. pachyderma (s.)*	18420	180/170	22070	KIA6128
PS2876-2	133	*N. pachyderma (s.)*	19750	120	23480	KIA6129
PS2876-2	178	*N. pachyderma (s.)*	22030	180/170	25830	KIA6130
PS2876-2	257.5	*N. pachyderma (s.)*	28490	360/340	32390	KIA6131
PS2876-2	288.5	*N. pachyderma (s.)*	29100	330/310	32900	KIA7577
PS2876-2	321.5	*N. pachyderma (s.)*	31500	350/340	35150	KIA7578
PS2876-2	356.5	*N. pachyderma (s.)*	49830	5350/3180	51170	KIA7579
PS2887-2	13.5	*N. pachyderma (s.)*	9630	60	10960	KIA4647
PS2887-2	19.5	*N. pachyderma (s.)*	9660	55	10960	KIA7575
PS2887-2	22.5	*N. pachyderma (s.)*	11225	60	13140	KIA7576
PS2887-2	25.5	*N. pachyderma (s.)*	12360	60	14270	KIA7574
PS2887-1	25.5	*N. pachyderma (s.)*	11910	80	13820	KIA6114
PS2887-1	33.5	*N. pachyderma (s.)*	14900	100	17710	KIA6115
PS2887-1	35.5	*N. pachyderma (s.)*	15470	110	18370	KIA6116
PS2887-1	40.5	*N. pachyderma (s.)*	15990	100	18960	KIA4648
PS2887-1	43.5	*N. pachyderma (s.)*	16690	100	19770	KIA6117
PS2887-1	45.5	*N. pachyderma (s.)*	17380	110	20560	KIA6118
PS2887-1	52.5	*N. pachyderma (s.)*	18040	150	21320	KIA6119
PS2887-1	69.5	*N. pachyderma (s.)*	23830	230	27730	KIA4649
PS2887-1	84.5	*N. pachyderma (s.)*	41660	1790/1460	44260	KIA6120
PS2887-1	96.5	*N. pachyderma (s.)*	43580	2190	45480	KIA4650
OD-041-04	2.5	*N. pachyderma (s.)*	5120	30	5900	KIA4656
OD-041-04	6.5	*N. pachyderma (s.)*	8910	50	9960	KIA4657
OD-041-04	10.5	*N. pachyderma (s.)*	10630	70	12560	KIA4658
OD-041-04	14.5	*N. pachyderma (s.)*	16630	130	19560	KIA4659
OD-041-04	14.5	*O. umbonatus*	16620	130	19540	KIA6111
OD-041-04	23.5	*N. pachyderma (s.)*	24670	260/250	28690	KIA4661
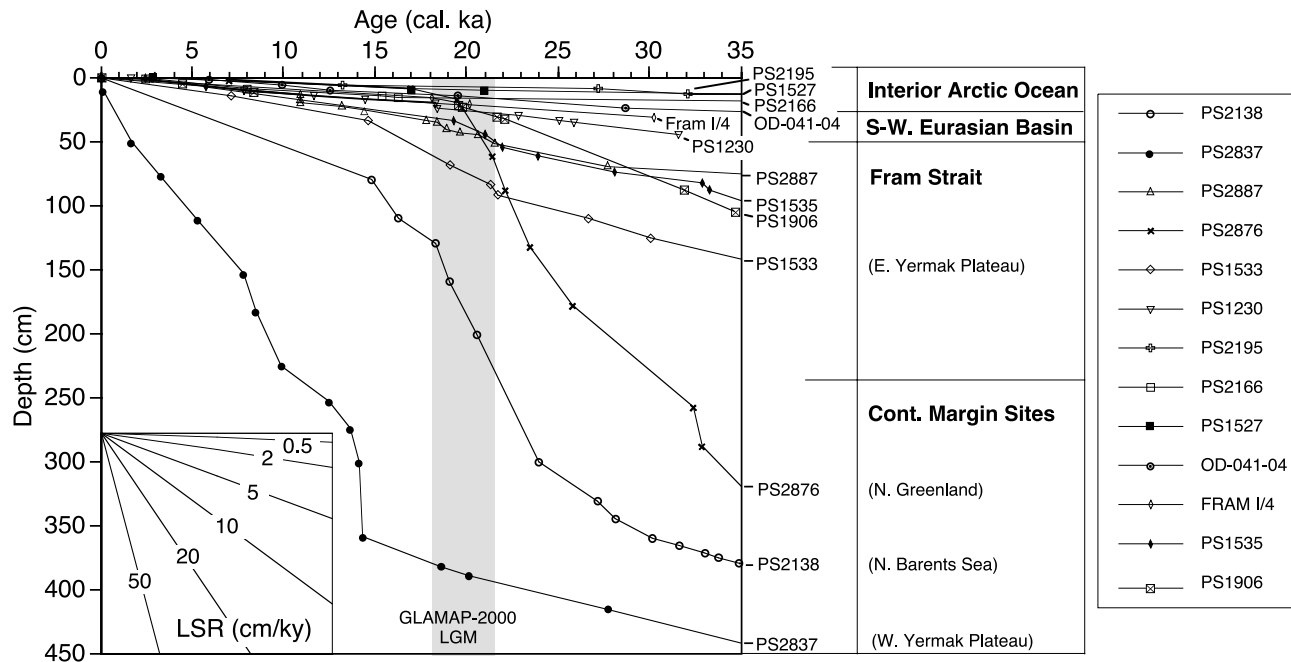
Figure 3. Depth-age plot of key cores based on radiocarbon dates converted into calendar years. The inset in the lower left corner shows the range of linear sedimentation rates (LSR) that can be derived from the inclination of the connecting lines between age control points. The GLAMAP 2000 LGM (21.5–18 cal. ka) time slice is indicated. Sources for radiocarbon datings are *Köhler* [1992] (PS1527), *Markussen* [1986] (FRAM I/4), and *Knies and Stein* [1998] (PS2138). Others are listed in Table 2.

mass with a high reservoir time. At high-resolution site PS2644 in the Denmark Strait (under the East Greenland Current), *Voelker et al.* [1998] determined benthic foraminifer ages to be up to 1600 years younger than the respective planktic foraminifer ages during the LGM and the initial deglaciation. If differential bioturbation for benthic and planktic foraminifers can be ruled out, this suggests that "old" subsurface water influenced the planktic ages whereas "young" glacial intermediate to deep water gave the benthic species their apparently younger age. We do not have evidence that such old subsurface waters originated from the interior Arctic Ocean, which was characterized by low-$\delta^{18}O$ surface waters. Sites from the southwestern Eurasian Basin (e.g., PS2876, OD-041-04, and Fram I/4) show stable, high $\delta^{18}O$ values during the LGM period, and at site OD-041-04 the planktic and benthic ages in the LGM interval are almost identical (Table 2). This indicates that the oceanographic situation here was different than the situation at site PS2644, although we cannot finally exclude the possibility that both planktic and benthic ages are biased by old water masses. In the eastern and central Fram Strait and on the outer Yermak Plateau the $\delta^{18}O$ values of the LGM interval are high and rather constant in the range of 4.5–4.8‰. In cores from the western Fram Strait, equally high $\delta^{18}O$ values are found only in the early and late LGM

interval. These high values are in the same range as the ones reported for the Nordic Seas LGM [*Sarnthein et al.*, 1995] and thus likely represent water of Atlantic origin advected to the north. Along the northern Barents Sea slope, mean $\delta^{18}O$ values are in the range of 4.2–4.5‰ with peak values of about 4.5–4.8‰. The slightly lower values observed in that region may imply that surface and subsurface waters were occasionally influenced by some meltwater supply from the adjacent Barents Sea Ice Sheet. The cores from the southwestern Eurasian Basin (up to about 84°N) have a characteristic MIS 2 interval with high $\delta^{18}O$ values in the LGM comparable to the values in the eastern-central Fram Strait. Even core OD-041-04, from the southern flank of the Gakkel Ridge (84°N, 11°E), has $\delta^{18}O$ values up to 4.8‰ in a planktic foraminiferal abundance peak that has been dated to 16.6 ^{14}C ka. In core Fram I/4, from about the same latitude in the Fram Basin between the Morris Jesup Rise and the Gakkel Ridge, the LGM interval shows values in the range 4.4–4.6‰. From about 85°N and further into the central Arctic Ocean and the Amerasian Basin, MIS 2 becomes extremely condensed, represented by only a few cm downcore [cf. *Nørgaard-Pedersen*, 1997; *Darby et al.*, 1997; *Poore et al.*, 1999]. The peak glacial $\delta^{18}O$ values appear to decrease toward lowest values (≤ 2.5‰) in the central Arctic Ocean (Table 1). Due to bioturbation and

Notes to Table 2

[a]A 400 year reservoir correction was applied to all AMS-^{14}C ages.

[b]The radiocarbon ages were converted to calendar ages by the CALIB 4.1.2 calibration program [*Stuiver and Remer*, 1993; *Stuiver et al.*, 1998] and, beyond 20.3 ^{14}C ka, by the age shift curve given by *Voelker et al.* [1998].
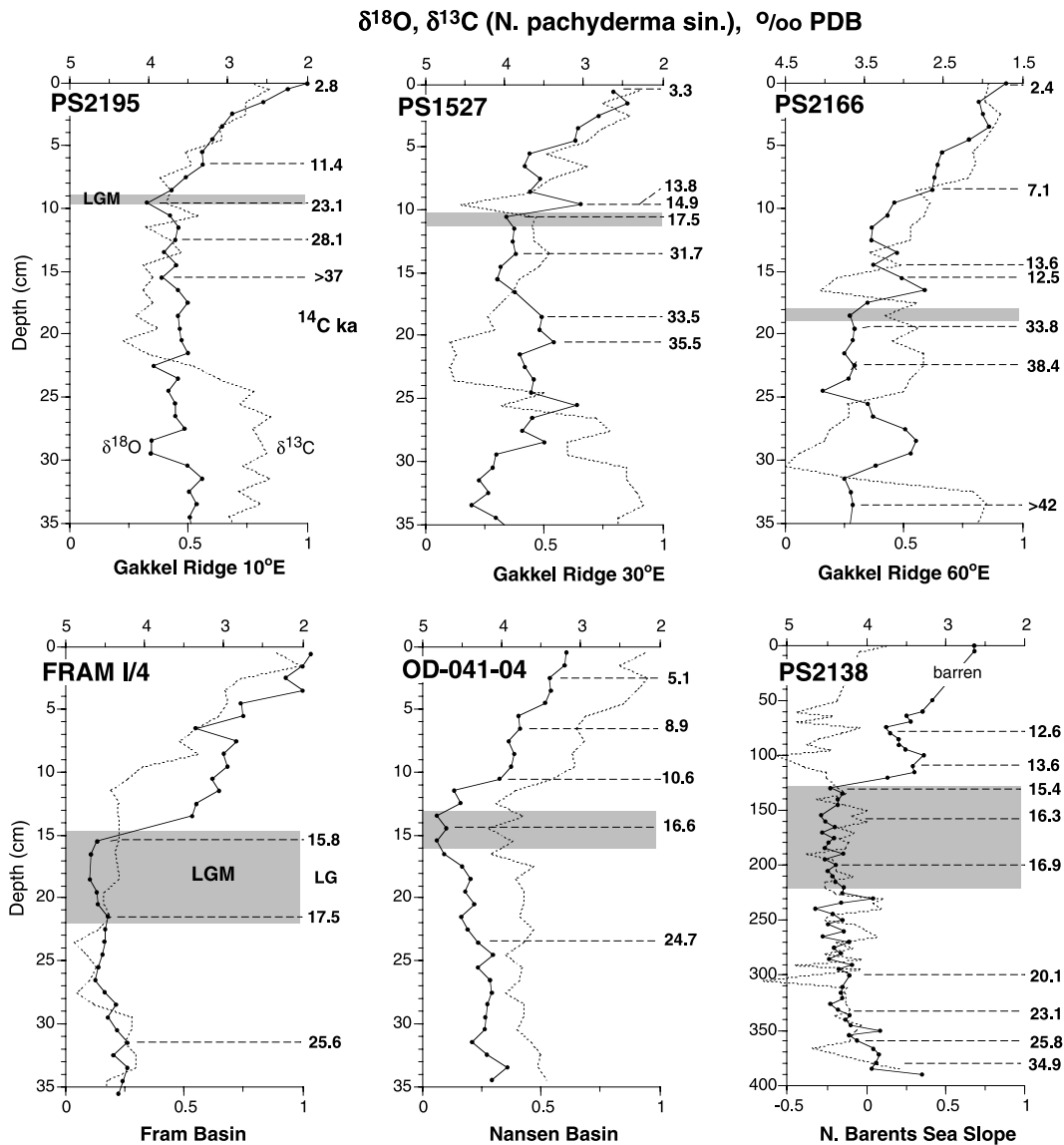
Figure 4. *N. pachyderma* (s) $\delta^{18}O$ (solid line, upper scale) and $\delta^{13}C$ (dotted line, lower scale) isotope records. Radiocarbon dates in ^{14}C kyr BP are shown along the right margin of the diagrams. The GLAMAP 2000 LGM (18−15 ^{14}C ka) time slice is indicated by shaded bars. The record of PS1527 is from *Köhler* [1992], FRAM I/4 is from *Markussen* [1986], and the PS2138 record is from *Knies and Stein* [1998].

limited sample resolution, the isotope values may, at best, be average proxies of MIS 2 conditions. Low $\delta^{18}O$ signals from the last deglacial probably bias the measured LGM values to some extent. However, it is characteristic for central Arctic Ocean radiocarbon-dated records that the MIS 2 last deglacial transition is marked by a pronounced decrease of $\delta^{18}O$ and $\delta^{13}C$ values associated with a sudden increase of ice rafted debris content [*Stein et al.*, 1994; *Nørgaard-Pedersen*, 1997; *Nørgaard-Pedersen et al.*, 1998]. The abrupt and ubiquitous change in stable isotope values and sediment characteristics observed suggests that bioturbational mixing has not severely influenced the central Arctic proxy records obtained in this study.

[16] We have compiled maps of the planktic $\delta^{18}O$ distribution for the GLAMAP 2000 LGM time slice from the Fram Strait to the central Arctic (Figure 6). Due to the extremely low sedimentation rates north of 85°N, mean and maximum values (Figures 6a and 6b) are identical here. However, remarkable differences between the mean and maximum data sets are evident in the area along the northern Barents Sea and Northeast Greenland slopes. Both areas may episodically have been under the influence of isotopically light meltwater influx from the adjacent ice sheets, causing more variable isotopic records. If the decrease of $\delta^{18}O$ values by several permille toward the north accurately reflects the oceanographic conditions during the LGM, and bioturbational mixing of signals can be neglected, the data reveal a gradient in surface ocean salinity comparable to today (3−4 salinity units from the Barents Sea continental margin to the North Pole [c.f. *Spielhagen and Erlenkeuser*, 1994]).
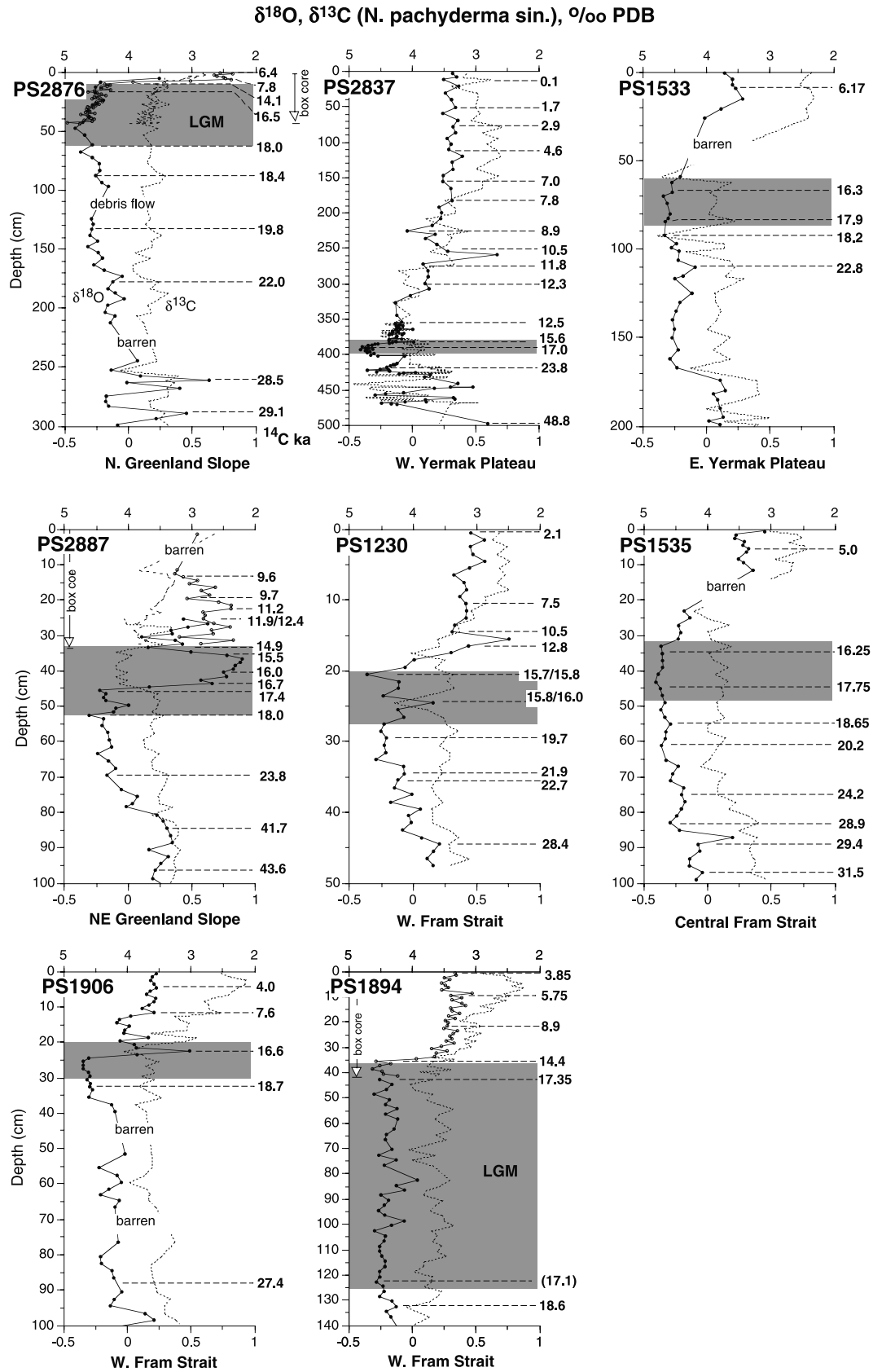
$\delta^{18}O$, $\delta^{13}C$ (N. pachyderma sin.), ‰ PDB

Figure 4.   (continued)

δ18O (N. pachyderma sin.), º/oo PDB
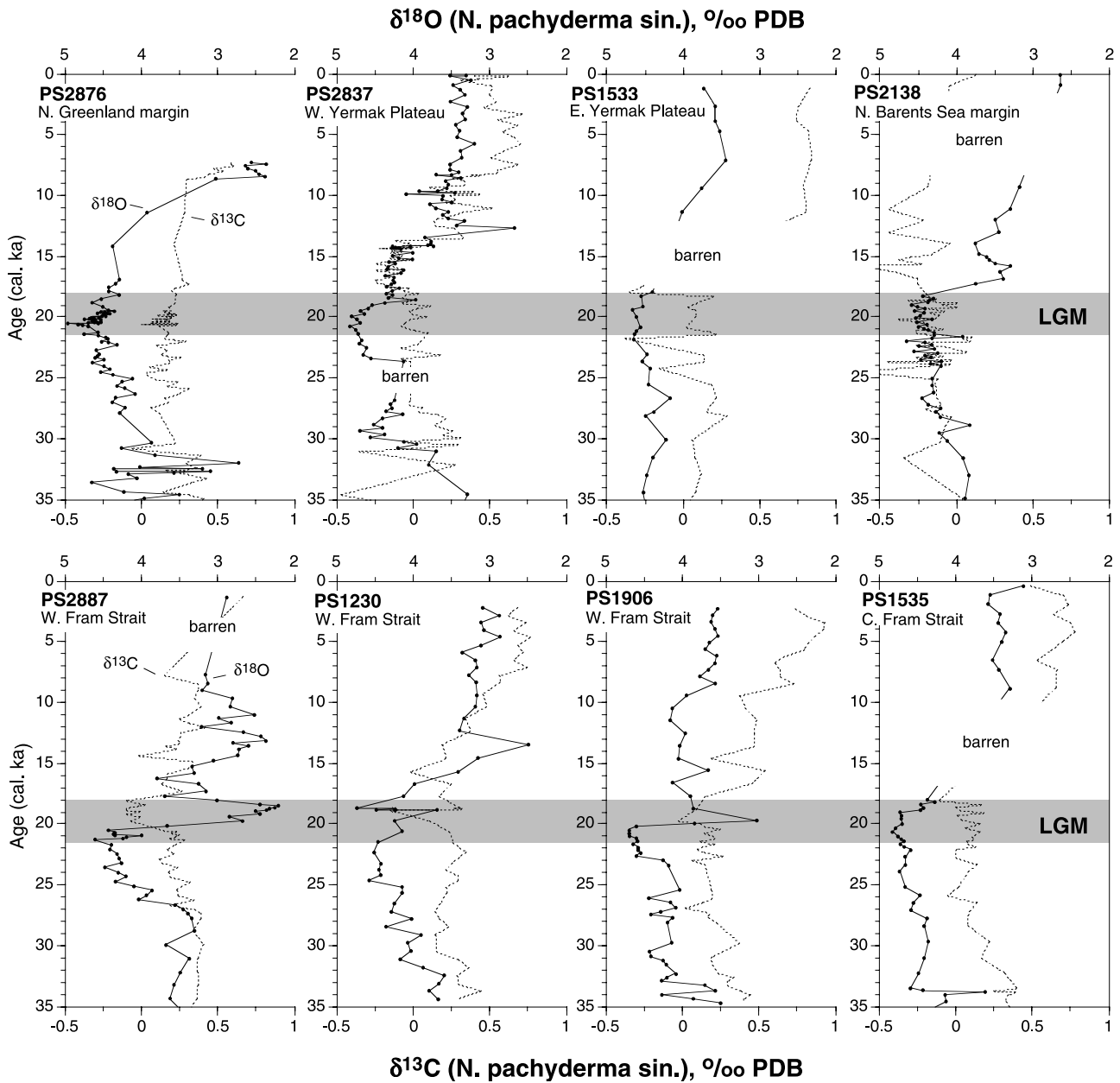

δ13C (N. pachyderma sin.), º/oo PDB

Figure 5. High-resolution stable isotope records (*N. pachyderma* (s)) versus age (cal. ka) from two transects across the northern Barents Sea slope-Yermak Plateau-northern Greenland slope and along the western-central Fram Strait, respectively. The GLAMAP 2000 LGM (21.5–18.0 cal. ka) time slice is indicated. The PS2138 record is from *Knies and Stein* [1998]. Note that a prominent low-δ18O spike characterizes the western Fram Strait records about 20–19 cal. ka.

However, salinities might have been offset by melting and refreezing of sea ice. In addition, different habitat levels of planktic foraminifers in salinity-stratified waters also make direct derivation of paleosalinities problematic [*Kohfeld et al.*, 1996; *Bauch et al.*, 1997; *Nørgaard-Pedersen*, 1997].

4.3. Planktic Foraminiferal Abundance and Flux Estimates

[17] In general, high abundances of planktic foraminifers (>125 μm) are found in the LGM interval in the Fram Strait and the southwestern Eurasian Basin (Figure 7). A charac-

teristic peak with abundances of about 4000–6000 specimens g⁻¹ sediment culminates about 20–19 cal. ka. In general, foraminiferal abundances are lower in the early part of the LGM time slice. Another peak with similar abundance levels in the Fram Strait and Yermak Plateau region is found in the interval 30–27 cal. ka. These two events correspond to the glacial "high productive zones" 1 and 2 first reported from the eastern Fram Strait and the Norwegian Sea by *Hebbeln et al.* [1994] and *Dokken and Hald* [1996]. Between these two episodes, much lower foraminiferal abundances are found, with minimum values reached
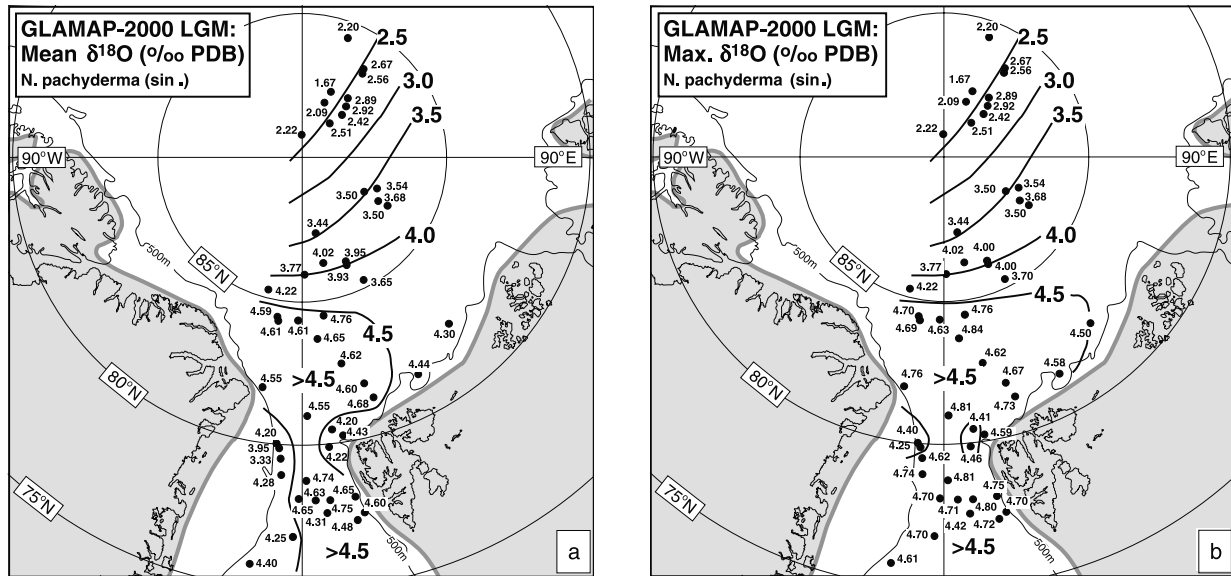
Figure 6. Distribution of (a) mean $\delta^{18}O$ values and (b) maximum $\delta^{18}O$ values of *N. pachyderma* (s) for the GLAMAP 2000 LGM time slice (21.5–18.0 cal. ka) in Fram Strait to central Arctic records. Source information on specific records is given in Table 1.

in the time interval 25–24 cal. ka. In the Yermak Plateau records, this minimum is even more pronounced due to carbonate dissolution and dilution by terrigenous material (note high coarse fraction content in PS2837). In the region further to the north, the LGM foraminiferal abundance peak can be traced across the western Nansen Basin up to the Gakkel Ridge (cores OD-041-04 and PS2206). It is also present in the Fram Basin (Fram I/4 core) [*Markussen*, 1986; *Zahn et al.*, 1985] and on the slope off North Greenland (core PS2876). From 84°N to 85°N, in the southwestern Eurasian Basin, the high abundance of planktic foraminifers in the LGM interval is lost and to the north only a few hundred foraminifers g^{-1} characterize the MIS 2 sediment [cf. *Nørgaard-Pedersen*, 1997; *Nørgaard-Pedersen et al.*, 1998]. In fact, in most cores north of 85°N, the LGM interval exhibits a pronounced minimum in foraminiferal abundances for the last 35 kyr.

[18] In order to use the planktic foraminiferal abundance records as a proxy for planktic productivity, we have calculated flux estimates (specimens >125 µm m^{-2} yr^{-1}) for selected records with a reliable stratigraphy constrained by radiocarbon dates (Figure 8). While some of these records have been influenced by dissolution in the Holocene and the deglacial period, the preservation of tests seems to be very good in all cores through the LGM interval. It should also be emphasized that linear interpolation between age control points and the resulting (unrealistic) jagged nature of the bulk sediment accumulation rate records considerably biases the foraminiferal flux records. In many cases, especially where the abundance peaks of planktic foraminifers have been dated, and where apparently abrupt changes in sedimentation rates take place, the foraminiferal flux records are affected accordingly (e.g., over/under represented). Examples of such artificial peaks in the LGM interval are seen in core PS2876 (Figure 8).

[19] In spite of the above limitations, the flux records from the Fram Strait and the southwestern Eurasian Basin reveal that the LGM interval 22–19 cal. ka was characterized by relatively high productivity. The planktic foraminiferal flux decreased from about 25–35 specimens cm^{-2} yr^{-1} in the eastern-central Fram Strait (PS1535) and on the northern Svalbard Margin (PS1533) to about 5–10 specimens cm^{-2} yr^{-1} in the western Fram Strait (PS1230, PS2887), the northwestern Yermak Plateau (PS2837), and the southwestern Eurasian Basin (OD-041-04). These values are similar to the Norwegian Sea flux values for *N. pachyderma* (s) during the LGM [*Bauch*, 1993]. In many cases, the LGM flux values from these regions are higher than Holocene estimates. However, in several cases, the latter are biased by dissolution effects, causing lower apparent Holocene flux values.

[20] North of 85°N in the European sector (0–90°E), the flux estimates decrease to <0.2 specimens cm^{-2} yr^{-1} (cores PS2195 and PS2166 from the Gakkel Ridge) and indicate very low productivity. From the Lomonosov Ridge, comparably low MIS 2 productivity estimates have been reported from cores PS2177 and PS2185 [*Nørgaard-Pedersen et al.*, 1998]. Since the oxygen isotope values of *N. pachyderma* (s) in the LGM interval in these "low productive zone" cores are considerably different (0.5–2.5‰ lower) than the characteristically high values obtained from the "high productive zone" to the south (Figures 6 and 9), it seems unlikely that the foraminifers managed to drift hundreds of kilometers to the central Arctic sites. It is therefore assumed that the foraminifers found in the LGM interval of the central Arctic largely represent local production.

4.4. Ice-Rafted Debris Content

[21] Spatial changes of IRD (>500 µm) deposition in the Fram Strait to the central Arctic Ocean during the last

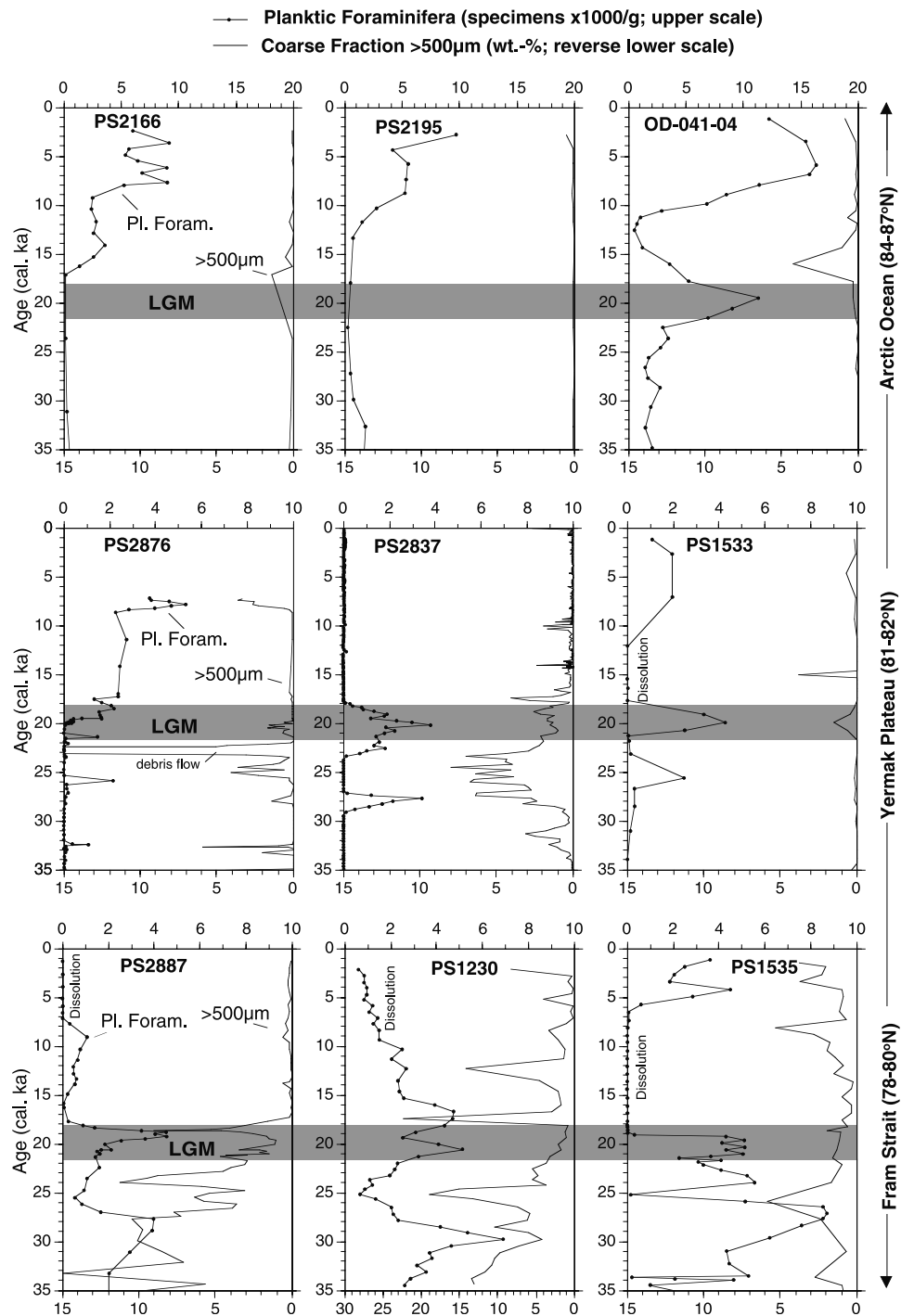**Figure 7.** Abundance records of planktic foraminifers (specimens 10^3 g^{-1} bulk sediment) and percentage coarse fraction and >500 μm (reverse lower scale) of key cores from the Fram Strait, the Yermak Plateau-North Greenland transect, and the interior Arctic Ocean. The GLAMAP 2000 LGM (21.5–18 cal. ka) time slice is indicated. Intervals with extremely low contents of planktic foraminifers due to dissolution are indicated (not during the LGM). The PS1533 record is from *Pagels* [1991] and the PS2166 and PS2195 records are from *Nørgaard-Pedersen et al.* [1998].

35 kyr are shown in Figure 7. Maxima of IRD contents in cores from the southern region were reached before the LGM, in the period 23–28 cal. ka. For this time interval, the records from the Fram Strait (PS1535, PS1230, PS2887) and the western Yermak Plateau (PS2837) show about 5–15% >500 μm whereas the subsequent LGM interval only has about 2–5% >500 μm. From earlier studies of Fram Strait cores it was concluded that the Svalbard-Barents
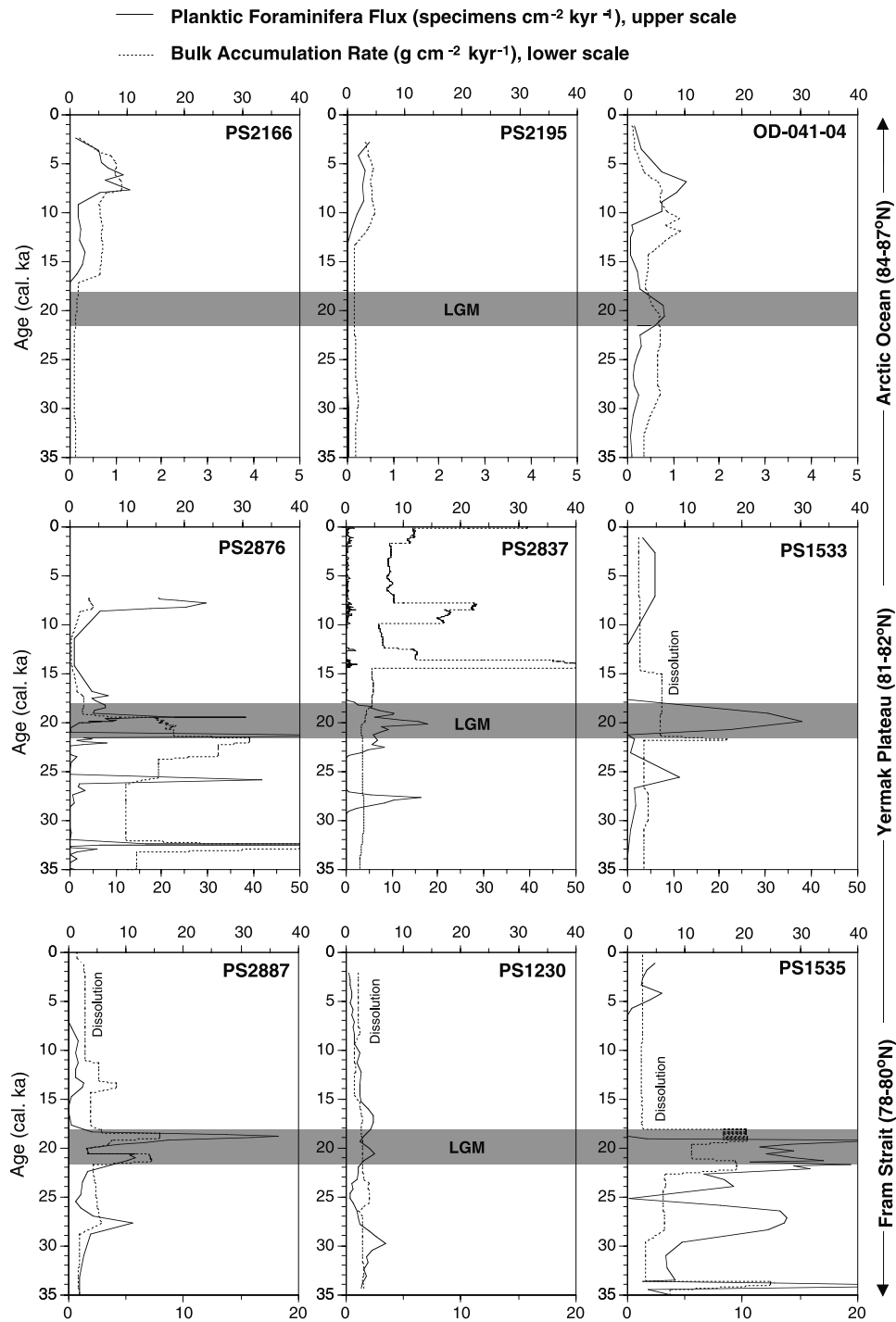
Figure 8. Planktic foraminiferal flux records (specimens cm^{-2} yr^{-1}) and bulk sediment accumulation rate records (g cm^{-2} kyr^{-1}). Note that the foraminiferal flux records become stretched (over/under represented; e.g., PS2837 at about 17.5 cal. ka., and PS2876 at about 19.5 cal. ka. and 21.5 cal. ka), when apparently abrupt changes in accumulation rate take place.

Sea Ice Sheet build-up occurred within a few thousand years prior to the LGM [*Hebbeln et al.*, 1994; *Elverhøi et al.*, 1995; *Landvik et al.*, 1998; *Knies et al.*, 2001]. Although strong IRD input indicating enhanced iceberg release during initial deglaciation along the northern Barents Sea conti-

nental margin began during the youngest part of the GLAMAP 2000 LGM (15.4 ^{14}C) [*Knies et al.*, 2001], the meltwater input to the Arctic Ocean prior to 15.0 ^{14}C ka, as indicated by isotopic records, was restricted to the ice-proximal area [cf. *Nørgaard-Pedersen et al.*, 1998].
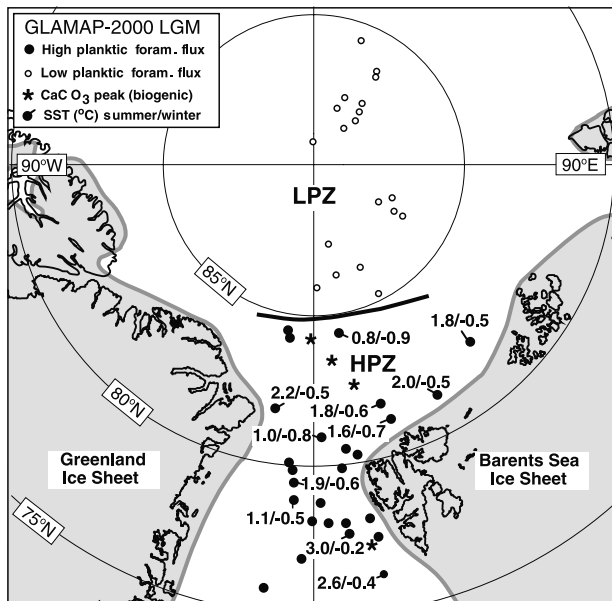
Figure 9. Distribution of mean summer and winter sea surface temperatures (SST) estimated for the GLAMAP 2000 LGM time slice on selected records [from *Pflaumann et al.*, 2003]. Also shown are LGM records with a high planktic foraminiferal flux (solid circles) and/or a prominent biogenic CaCO$_3$ peak (HPZ, high productive zone) and the interior Arctic sites north of 85°N (open circles) characterized by an extremely low flux of planktic foraminifers (LPZ, low productive zone). Sources are listed in Table 1.

[22] In the interior Arctic Ocean (e.g., OD-041-04, PS2195, PS2166, and cores discussed by *Nørgaard-Pedersen et al.* [1998]), the IRD content in MIS 2 is very low (<1%) and peak values are associated with the last deglaciation (<17 cal. ka). Although the small numbers of IRD grains in the individual samples from this region limit the statistical significance, the generally low IRD flux in the central Arctic Ocean during the LGM indicates that melting was strongly restricted [*Darby et al.*, 2002] or that only few icebergs reached that region.

4.5. Sea Surface Temperature Estimates

[23] Based on planktic foraminiferal assemblage data, *Pflaumann et al.* [2003] reconstructed mean summer sea surface temperature (SST) for the glacial North Atlantic to Arctic Ocean region. We briefly present their results for the GLAMAP 2000 LGM time slice in our study area here because they were obtained from cores also used for our study and because they can be used to corroborate our results (results for the EPILOG LGM are very similar).

[24] Summer SST estimates for the GLAMAP 2000 LGM time slice in the Fram Strait and the southwestern Eurasian Basin are in the range 0.8–3.0°C (average 1.8°C), and the mean winter temperature estimates are −0.9 to −0.2°C (average −0.5°C) [*Pflaumann et al.*, 2003]. The summer SSTs at selected core sites in the western Fram Strait and the southwestern Eurasian Basin were only slightly lower (by 1–2°C) than the values estimated for the Norwegian Sea

[*Weinelt et al.*, 1996; *Pflaumann et al.*, 2003]. As noted by *Weinelt et al.* [1996], these temperature estimates may be too high because the SIMMAX and other transfer equations tend to overestimate the actual values (up to 3°C) in frontal systems where relatively warm, high density surface water with ''warm'' planktic foraminifers submerges below colder, low-salinity and low-density surface water. This is the situation in the present western Fram Strait and the southwestern Eurasian Basin, and may also have been the case in this region during the LGM (see discussion below). For further discussion of the error range in SST estimates, see *Sarnthein et al.* [2003b].

5. Discussion

5.1. Last Glacial Maximum Arctic Ocean Paleoceanography: Regional Variability

[25] The data presented above document considerable spatial differences in environmental proxies along a transect from the Fram Strait to the central Arctic Ocean. We have been able to map out three different regions A–C, characterized by different sedimentation regimes and surface ocean properties during the LGM (Figure 10). In the following discussion these regions will be described in terms of paleoceanographic conditions.

5.1.1. Area A

[26] The eastern Fram Strait and the northern Barents Sea margin area were characterized during the LGM by high sedimentation rates (2–10 cm kyr^{-1}) and comparatively high fluxes of planktic foraminifers and IRD. Such environments are presently found in areas of seasonally changing ice cover as the central Fram Strait [*Hebbeln and Wefer*, 1991]. The high-δ^{18}O values of *N. pachyderma* (s) and the summer SST estimates of about 1.6–3.0°C suggest a strong inflow of Atlantic Water. However, as noted earlier, the paleotemperatures may be overestimated, and the deeper calcifying depths of *N. pachyderma* (s) may imply that the indicated paleotemperatures signify a subsurface Atlantic water mass.

5.1.2. Area B

[27] The adjacent region, the western Fram Strait and the southwestern Eurasian Basin up to about 84–85°N, was characterized by lower sedimentation rates (1–3 cm kyr^{-1}), a moderately high flux of planktic foraminifers and IRD, high δ^{18}O values of *N. pachyderma* (s), and summer SST estimates slightly lower than in area A. We suppose that area B was under the steady influence of Atlantic subsurface waters advected from area A.

5.1.3. Area C

[28] The central Arctic Ocean (north of 85°N in the Eurasian Basin) was characterized by extremely low sedimentation rates (mm kyr^{-1}) and low fluxes of planktic foraminifers and IRD suggesting a perennially extensive ice cover.

[29] Our results support earlier conclusions that the influence of advected Atlantic Waters played a much larger role on the character of the ice cover and the sedimentation regime in the Eurasian Basin during the LGM than proposed by the *CLIMAP Project Members* [1981] Working Group. *Hebbeln et al.* [1994] and *Dokken and Hald* [1996] presented evidence for a meridional circulation pattern and
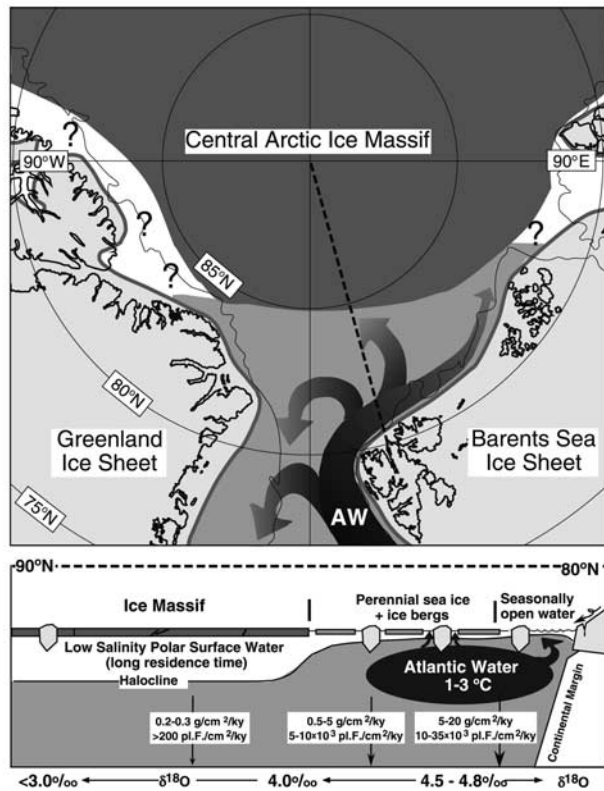
Figure 10. Simplified model of ice cover character and surface ocean conditions in the Fram Strait-central Arctic Ocean region during the LGM. On the latitudinal transect from the N. Svalbard continental margin to the North Pole, related proxy data as sedimentation rates, planktic foraminiferal flux, planktic δ^{18}O values, and mean summer SST values of the Atlantic Water mass are shown. Advection and recirculation of relatively warm and saline Atlantic Water in the Fram Strait-southwestern Eurasian Basin caused an open ice cover and a relatively high flux of biogenic and lithic material. Polynyas may have characterized the Barents Sea continental margin. From about 85°N and further into the interior Arctic, evidence indicates that ice cover was permanently thick, resting upon cold, low-salinity halocline waters. This may explain the extreme low interior Arctic flux values.

seasonally ice-free waters during most of the LGM in the Norwegian Sea and the eastern Fram Strait. They also concluded that open water conditions were an important regional moisture source for the rapid build-up of the Barents Sea Ice Sheet. *Knies et al.* [1999] found evidence for a continuation of the open water area along the northern Barents Sea margin (to at least 45°E). They suggested that a coastal polynya was kept open by katabatic winds blowing off the adjacent ice sheet. An inflow of subsurface Atlantic Water may have supported these seasonally ice-free conditions. The high flux of biogenic calcite (mostly foraminifers) found in the Barents Sea margin cores was explained by *Knies et al.* [1999] as a result of high lithogenic fluxes from the ice margin and a subsequent intensive supply of nutrients

induced by upwelling of Atlantic Water. The present study documents that relatively high fluxes of planktic foraminifers in the LGM interval also occurred further off the Svalbard-Barents Sea continental margin. The ubiquitous high δ^{18}O values of *N. pachyderma* (s) in the Fram Strait and the southwestern Eurasian Basin (Figure 6), as well as the spatial pattern of stable paleotemperature estimates (Figure 9), suggest that a homogeneous near surface water mass characterized the entire Fram Strait and the southwestern Eurasian Basin up to 84–85°N (including the northern Barents Sea margin). The higher sedimentation rates and planktic foraminifer and IRD fluxes in area A suggest that this region must have been characterized repeatedly by at least seasonally open-water conditions, a relatively high biogenic productivity and abundant drifting icebergs. The latter probably originated from the Barents Sea Ice Sheet [*Knies et al.*, 2000], which also supplied some meltwater to the area, as indicated by slightly lower δ^{18}O values along the northern Barents Sea margin. The Scandinavian Ice Sheet was an additional IRD source during the high productive periods of Atlantic Water advection [*Hebbeln et al.*, 1994; *Andersen et al.*, 1996; *Vogt et al.*, 2001]. According to the reconstructions of *Pflaumann et al.* [2003] and *Sarnthein et al.* [2003b], open waters in summer may have reached up to 78°N in the eastern Fram Strait, while the rest of the Fram Strait and the Arctic Ocean were covered by perennial ice. In fact, this may have been the normal situation during average summers in the LGM. Ice conditions in region A may have been strongly variable, especially north of 78°N, where they probably resembled the modern situation in the southern Nansen Basin north of Svalbard and the Barents Sea continental margin. Our observations (N. N.-P., R. F. S.) from research icebreaker cruises over the last decade suggest that in some years (e.g., 1993) the summer margin of dense sea ice remained along the upper Barents Sea continental margin at 81°N, whereas in other years (e.g., 2001) the southern Nansen Basin as far north as 83–84°N was totally ice-free. The significant differences in sedimentary fluxes below both regimes [*Hebbeln and Wefer*, 1991] result in the overrepresentation of sedimentary particles (e.g., planktic foraminifers) in regions characterized by marked interannual variation in ice coverage. For this reason, our environmental reconstruction of the LGM (Figure 10) may represent the exceptional years rather than the typical years, with seasonally open water areas north of 78°N when most of the sedimentary particles were deposited. We note that this interpretation is not in conflict with the results of *Pflaumann et al.* [2003] and *Sarnthein et al.* [2003b].

[30] The decrease in foraminifer fluxes and sedimentation rates from areas A to B indicates that open water conditions in B were rare and may have been restricted to exceptional years. The ice cover may have been similar to modern conditions in the interior Arctic Ocean, where open waters occur only as leads between moving sea ice fields and make up less than 5% of the area. The planktic foraminifers in LGM samples from area B may to a large extent have been carried there by Atlantic Waters from the south. Such transport may, in part, account for the pronounced oxygen isotopic homogeneity between areas A and B. We propose

that subsurface Atlantic Water descended below a cold Arctic halocline surface layer with a perennial sea ice cover, a situation comparable to the present conditions in the region. The relatively high bulk sediment accumulation rates and moderately high IRD fluxes in the SW Eurasian Basin suggest that erratic-bearing icebergs were drifting and melting in the region. Based on detailed IRD analyses of core PS1230 in the western Fram Strait, *Darby et al.* [2002] concluded that these icebergs originated from northern Canada and Greenland. The tentative flux values for the interior Arctic (area C) are at least a factor of 10 lower and indicate that deposition of IRD was limited there. During the LGM, icebergs from northern Canada may have crossed this region, but extremely low melt-out rates prevented significant IRD contributions [*Darby et al.*, 2002].

[31] The sediment properties from area C suggest that this area was most likely covered by thick sea ice which only very rarely broke up and significantly limited planktic productivity and sedimentation in general [*Nørgaard-Pedersen et al.*, 1998; *Darby et al.*, 1997]. Peak glacial $\delta^{18}O$ values of *N. pachyderma* (s) decrease by several permille from the southwestern Eurasian Basin toward the interior Arctic. If bioturbation influence has been insignificant, these observations suggest that, similar to today, an upper low-salinity layer characterized the central Arctic Ocean during the LGM. Assuming a stable halocline, sea surface temperatures were most likely (as today) close to the freezing point (i.e., $-1.8°C$). Cores from the Northwind Ridge and the Chukchi Plateau (Amerasian Basin) are barren of foraminifers in the glacial interval [*Darby et al.*, 1997; *Phillips and Grantz*, 1997], suggesting an even thicker and more coherent sea ice cover, which was of a sufficient thickness to reduce solar irradiance to levels that precluded photosynthesis.

5.2. Arctic Ocean Salinity Distribution and Halocline Properties During the Last Glacial Maximum

[32] Details of the spatial distribution of planktic $\delta^{18}O$ values for the LGM time slice are somewhat different from the distribution of core top values which reflect late Holocene conditions. The core top values show a gradual decrease from the Barents Sea margin to the interior Arctic [*Spielhagen and Erlenkeuser*, 1994], whereas the LGM values show a steep gradient only north of 85°N. These patterns probably represent different salinity distributions and halocline properties of near-surface water masses. Our data suggest that, if a low-salinity surface layer was present in the southwestern Eurasian Basin, it may have been considerably thinner than today (<50 m), leaving little or no trace in the proxies. The reasons for the apparently low salinity of the LGM central Arctic Ocean surface waters are somewhat elusive. Little is known about the discharge of Siberian rivers during that time. Paleobotanical data [*Tarasov et al.*, 1999] and evidence for a reduced hydrologic cycle as revealed by ice core data [*Alley et al.*, 1993] suggest dry conditions and a reduced freshwater runoff. On the other hand, the lack of a large-scale glaciation in northern Siberia [*Svendsen et al.*, 1999] left pathways for the large river systems draining northern Asia, and filled-in paleoriver troughs on the Siberian shelves down to about 100 m below present sea level [*Kleiber and Niessen*, 1999] indicate active erosion from river activity even during the glacial sea level low stand. We interpret the abrupt drop of flux values at 85°N as indicative of a pronounced stable boundary between areas of different ice covers and water masses. The extensive ice cover north of 85°N may have inhibited mixing of the uppermost waters from wind action, and the lack of an Atlantic Water inflow may have allowed the establishment of a thick, stable layer of low salinity surface water. Due to the stability and slow exchange with more southerly areas, the residence time of the freshwater component may have been much longer than at present (only 7–15 years) [*Schlosser et al.*, 1994]. Maintenance of the interior Arctic halocline implies, however, that there was a continuous source of freshwater for the Arctic Ocean.

5.3. Last Glacial Maximum Atlantic Water Impact: Why So Strong?

[33] The question remains: Why was the impact of Atlantic Water so strong in the Fram Strait and the southwestern Eurasian Basin region despite the fact that the total amount of Atlantic Water advected to the Nordic Seas was probably lower than at present [*Seidov and Haupt*, 1997; *Kuijpers et al.*, 1998; *Lassen et al.*, 1999]? From our data and the paleoenvironmental reconstruction presented above, we speculate about some specific factors supporting and maintaining the paleoceanographic scenario during the LGM:

[34] 1. Funneling of the Atlantic Water through the Fram Strait took place at a time when the Barents Sea branch (presently transporting roughly 50% of all Atlantic Water to the Arctic Ocean) did not exist due to an ice sheet and lowered sea level. If we arbitrarily assume a 50% reduction of Atlantic Water advection to the Fram Strait during the LGM, the total volume passing through the strait would have been the same as today.

[35] 2. A limited freshwater supply to the Arctic Ocean (apart from melting icebergs) must have caused a progressive weakening of its halocline structure in the SW Eurasian Basin facing the Fram Strait. Shallowing of the Atlantic Water layer and "erosion" of the halocline waters may have been responsible for a locally enhanced oceanic heat flux to the surface mixed layer and a reduction of the sea ice cover.

[36] 3. Recirculation of Atlantic Water in the Fram Strait and the adjacent Arctic Ocean may have played an even larger role than today. At present, about 50% of the Atlantic Water advected to the eastern Fram Strait turns westward and southward as a subsurface current under the East Greenland Current, while the other 50% enters the Arctic Ocean [*Bourke et al.*, 1988; *Rudels et al.*, 1994]. If during the LGM the surficial outflow of low-salinity water in the western Fram Strait was limited due to reduced river run-off to the Arctic Ocean, recirculating Atlantic Water may have had a stronger impact on the surface ocean environment.

[37] 4. Open water areas (polynyas) along ice sheet margins may have been maintained (to some extent even outside the summer season) by strong katabatic winds from the adjacent Barents Sea Ice Sheet and may have caused upwelling of Atlantic Water and a high biological productivity. As suggested earlier by *Veum et al.* [1992] and *Dokken and Hald* [1996] for the LGM in the Norwegian Sea and the

western Fram Strait, brine formation associated with sea ice production could have caused the formation of dense intermediate and deep waters and established some local to regional convection, which in turn would have promoted northward flow of Atlantic Water at the (sub)surface. Abundant drifting large icebergs with a draft of several hundred meters may even have caused some minor local upwelling along their margins by stirring Atlantic Water to the surface.

5.4. Temporal and Regional Comparison

[38] The apparent LGM paleoenvironmental pattern of water masses and ice cover character can be linked to covariable factors such as the northward advection and extension of relatively warm and saline Atlantic surface-subsurface water, freshwater influx and halocline properties, dynamics of sea ice cover, and influence of ice sheet marginal processes. To some extent, our results for the LGM time slice, combined with earlier studies on Arctic Ocean records, show a pronounced similarity to the present environmental state; i.e., strong influence of Atlantic Water in the eastern Fram Strait and along the northern Barents Sea margin, and the occurrence of a low-salinity central Arctic surface layer. In other aspects, however, the LGM environment was considerably different. The extremely low sedimentation rates in the interior Arctic are evidence for a thicker and much more dense pack ice cover. The southwestern Eurasian Basin facing Fram Strait, in contrast, seems to have been a more dynamic environment due to the influence of recirculating Atlantic Water. In some respects, the early advocates for a glacial rigid "sea ice sheet" cover [*Broecker*, 1975; *Denton and Hughes*, 1981] over the Arctic Ocean may not have been so far off track. The major difference to those hypotheses and to the CLIMAP reconstruction, however, is that strong environmental gradients were present in the Arctic Ocean and that frontal zones characterized the southwestern Eurasian Basin under the strongest influence of Atlantic Water advection.

6. Conclusions

[39] Based on sedimentological and stable isotope data from a large number of well-dated sediment cores from the Eurasian sector of the Arctic Ocean, we have been able to characterize and map out regions of different paleoceanographic conditions for the LGM period. Low sedimentation rates in the central Arctic Ocean hamper accurate age control and only preliminary interpretations can be given here for that region.

[40] The *N. pachyderma* (s) $\delta^{18}O$ distribution for the LGM depicts two different regions of surface-subsurface ocean conditions in the Eurasian sector of the Arctic Ocean. High $\delta^{18}O$ values (4.5–4.8‰), indicative of near surface Atlantic Water masses, are found in the Fram Strait and in

the southwestern Eurasian Basin up to 84–85°N. Further north, within the central Arctic Ocean, a persistent trend toward lower $\delta^{18}O$ values (>2‰, similar to the present gradient) can be observed. We suggest that low-salinity halocline properties were maintained in the interior Arctic Ocean during the peak glacial. However, due to low temporal resolution, we stress that the data from the central Arctic Ocean are tentative and probably characterize average MIS 2 conditions rather than a specific LGM time slice.

[41] The isotopically distinct regions were characterized by marked differences in the flux of biogenic and lithogenic material. Comparatively high fluxes of planktic foraminifers, ice-rafted debris (IRD) and bulk sediment characterize the Fram Strait and the northern Barents Sea margin, suggesting ice-marginal to repeatedly open water conditions with drifting icebergs. In the southwestern Eurasian Basin up to 84–85°N, flux values were lower but still moderately high, and this region may have been characterized by an ice cover with some open leads in summer, similar to the present interior Arctic Ocean. Extremely low flux value estimates for the central Arctic Ocean north of 84–85°N suggest the existence of an extensive sea ice cover with low seasonal variation, limiting planktic productivity and IRD release.

[42] The impact of recirculating saline and relatively warm Atlantic Water over a large area of the southwestern Eurasian Basin was the decisive factor causing a break-up of the ice cover, relatively high sedimentation rates and a comparatively high planktic foraminiferal flux. This was probably enhanced by a limited freshwater supply to that region and a progressive weakening of its halocline structure by mixing and erosion from below by the subsurface Atlantic Water mass.

[43] We suggest that the central Arctic freshwater pool and its associated ice massif were trapped in the interior Arctic Ocean. Freshwater export rates through the Fram Strait region were probably much lower than the present-day values. Maintenance of the low-salinity layer may have been supported by yet unknown freshwater sources from the Siberian-North American margins.

References

Aagaard, K., and E. C. Carmack, The role of sea ice and other fresh water in the Arctic circulation, *J. Geophys. Res.*, *94*, 14,485–14,498, 1989.

Aagaard, K., and E. C. Carmack, The Arctic Ocean and climate: A perspective, in *The Polar Oceans and Their Role in Shaping the Global Environment*, *Geophys. Monogr. Ser.*, vol. 85, edited by O. M. Johannesen, R. D. Muench, and J. E. Overland, pp. 5–20, AGU, Washington, D. C., 1994.

Alley, R. B., et al., Abrupt increase in Greenland snow accumulation at the end of the Younger Dryas event, *Nature*, *362*, 527–529, 1993.

Andersen, E. S., T. M. Dokken, A. Elverhøi, A. Solheim, and I. Fossen, Late Quaternary sedimentation and glacial history of the western Svalbard margin, *Mar. Geol.*, *133*, 5–20, 1996.

Anderson, L. G., G. Björk, O. Holby, E. P. Jones, G. Kattner, K. P. Koltermann, B. Liljeblad,

R. Lindegren, B. Rudels, and J. H. Swift, Watermasses and circulation in the Eurasian Basin: Results from the Oden 91 expedition, *J. Geophys. Res.*, *99*(C2), 3273–3283, 1994.

Bauch, D., J. Carstens, and G. Wefer, Oxygen isotope composition of living *Neogloboquadrina pachyderma* (sin.) in the Arctic Ocean, *Earth Planet. Sci. Lett.*, *146*(1–2), 47–58, 1997.

Bauch, H., Planktische Foraminiferen im Europäischen Nordmeer—Ihre Bedeutung für die paläo-ozeanographische Interpretation während der letzten 600.000 Jahre, *Ber. Sonderforsch. 313*, 109 pp., Kiel Univ., Kiel, Germany, 1993.

Bourke, R. H., A. M. Weigel, and R. G. Paquette, The westward turning branch of the West Spitsbergen Current, *J. Geophys. Res.*, *93*(C11), 14,065–14,077, 1988.

Broecker, W. S., Floating glacial ice caps in the Arctic Ocean, *Science*, *188*, 1116–1118, 1975.

Carstens, J., and G. Wefer, Recent distribution of planktic foraminifera in the Nansen Basin, Arctic Ocean, *Deep Sea Res.*, *39*, 507–524, 1992.

Carstens, J., D. Hebbeln, and G. Wefer, Distribution of planktic foraminifera at the ice margin in the Arctic (Fram Strait), *Mar. Micropaleontol.*, *29*, 257–269, 1997.

Chapman, M. R., and M. A. Maslin, Low-latitude forcing of meridional temperature and salinity gradients in the subpolar North Atlantic and the growth of glacial ice sheets, *Geology*, *27*(10), 875–878, 1999.

Clark, D. L., and A. Hanson, Central Arctic Ocean sediment texture: A key to ice transport mechanisms, in *Glacial Marine Sedimentation*, edited by B. F. Molnia, pp. 301–330, Plenum Press, New York, 1983.

CLIMAP Project Members, The surface of the Ice-Age Earth, *Science*, *191*, 1131–1137, 1976.

CLIMAP Project Members, Seasonal reconstructions of the Earth's surface at the Last Glacial Maximum, *Geol. Soc. of Am. Map and Chart Ser.*, *MC-36*, Geol Soc. of Am., Boulder, Colo., 1981.

Darby, D. A., J. F. Bischof, and G. A. Jones, Radiocarbon chronology of depositional regimes in the western Arctic Ocean, *Deep Sea Res., Part II*, *44*(8), 1745–1757, 1997.

Darby, D. A., J. F. Bischof, R. F. Spielhagen, S. A. Marshall, and S. W. Herman, Arctic ice export events and their potential impact on global climate during the late Pleistocene, *Paleoceanography*, *17*(2), 1025, doi:10.1029/2001PA000639, 2002.

Denton, G. H., and T. J. Hughes, The Arctic Ice sheet: An outrageous hypothesis, in *The Last Great Ice Sheets*, edited by G. H. Denton and T. J. Hughes, pp. 437–467, John Wiley, New York, 1981.

de Vernal, A., C. Hillaire-Marcel, J.-L. Turon, and J. Matthiessen, Reconstruction of sea-surface temperature, salinity, and sea-ice cover in the northern North Atlantic during the last glacial maximum based on dinocyst assemblages, *Can. J. Earth Sci.*, *37*, 725–750, 2000.

Dickson, B., All change in the Arctic, *Nature*, *397*, 389–391, 1999.

Dokken, T., Last interglacial/glacial cycle on the Svalbard/Barents Sea margin, Ph.D. thesis, University of Tromsø, Tromsø, Norway, 1995.

Dokken, T. M., and M. Hald, Rapid climatic shifts during isotope stages 2–4 in the polar North Atlantic, *Geology*, *27*, 599–602, 1996.

Dyke, A. S., J. T. Andrews, P. U. Clark, J. H. England, G. H. Miller, J. Shaw, and J. J. Veillette, The Laurentide and Innuitian ice sheets during the Last Glacial Maximum, *Quat. Sci. Rev.*, *21*, 9–31, 2002.

Ehrmann, W., and J. Thiede, History of Mesozoic and Cenozoic sediment fluxes to the North Atlantic Ocean, *Contrib. Sedimentol.*, *15*, 109 pp., 1985.

Eiriksson, J., K. L. Knudsen, H. Haflidason, and J. Heinemeier, Chronology of late Holocene climatic events in the northern Atlantic based on AMS ^{14}C dates and tephra markers from the volcano Hekla, Iceland, *J. Quat. Sci.*, *15*(6), 573–580, 2000.

Elias, S. A., S. K. Short, C. H. Nelson, and H. H. Birks, Life and times of the Bering land bridge, *Nature*, *382*, 60–63, 1996.

Elverhøi, A., and A. Solheim, The Barents Sea ice sheet—A sedimentological discussion, *Polar Res.*, *1*, 23–42, 1983.

Elverhøi, A., E. S. Andersen, T. Dokken, D. Hebbeln, R. Spielhagen, J. I. Svendsen, M. Sørflaten, A. Rørnes, M. Hald, and C. F. Forsberg, The growth and decay of the late Weichselian ice sheets in western Svalbard and adjacent areas based on provenance studies of marine sediments, *Quat. Res.*, *44*(3), 303–316, 1995.

England, J., Coalescent Greenland and Innuitian ice during the Last Glacial Maximum: Revising the Quaternary of the Canadian High Arctic, *Quat. Sci. Rev.*, *18*(3), 421–456, 1999.

Funder, S., and L. Hansen, The Greenland ice sheet—A model for its culmination and decay during and after the Last Glacial Maximum, *Bull. Geol. Soc. Denmark*, *42*(2), 137–152, 1996.

Ganopolski, A., S. Rahmstorf, V. Petoukhov, and M. Claussen, Simulation of modern and glacial climates with a coupled global model of intermediate complexity, *Nature*, *291*, 351–356, 1998.

Grosswald, M. G., and T. J. Hughes, The Russian component of an Arctic ice sheet during the last glacial maximum, *Quat. Sci. Rev.*, *21*, 121–146, 2002.

Haflidason, H., J. Eiriksson, and S. Van Kreveld, The tephrochronology of Iceland and the North Atlantic region during the middle and late Quaternary: A review, *J. Quat. Sci.*, *15*(1), 3–22, 2000.

Hebbeln, D., Flux of ice-rafted detritus from sea ice in the Fram Strait, *Deep Sea Res., Part II*, *47*, 1773–1790, 2000.

Hebbeln, D., and G. Wefer, Effect of ice coverage and ice-rafted material on sedimentation in the Fram Strait, *Nature*, *350*, 409–411, 1991.

Hebbeln, D., and G. Wefer, Late Quaternary paleoceanography in the Fram Strait, *Paleoceanography*, *12*(1), 65–78, 1997.

Hebbeln, D., T. Dokken, E. S. Andersen, M. Hald, and A. Elverhøi, Moisture supply for northern ice-sheet growth during the Last Glacial Maximum, *Nature*, *370*, 357–360, 1994.

Hopkins, D. M., Aspects of the paleogeography of Beringia during the Late Pleistocene, in *Paleoecology of Beringia*, Academic, edited by D. M. Hopkins et al., pp. 205–217, San Diego, Calif., 1982.

Hughes, T. J., G. H. Denton, and M. G. Grosswald, Was there a late Würm Arctic ice sheet?, *Nature*, *266*, 596–602, 1977.

Jones, G. A., and L. D. Keigwin, Evidence from Fram Strait (78°N) for early deglaciation, *Nature*, *336*, 56–59, 1988.

Kageyama, M., O. Peyron, S. Pinot, P. Tarasov, J. Guiot, S. Joussaume, and G. Ramstein, The Last Glacial Maximum climate over Europe and Western Siberia: A PMIP comparison between models and data, *Clim. Dyn.*, *17*, 23–43, 2001.

Kleiber, H. P., and F. Niessen, Late Pleistocene paleoriver channels on the Laptev Sea Shelf—

Implications from sub-bottom profiling, in *Land-Ocean Systems in the Siberian Arctic: Dynamics and History*, edited by H. Kassens et al., pp. 657–665, Springer-Verlag, New York, 1999.

Knies, J., Spätquatäre Sedimentation am Kontinentalhang nordwestlich Spitzbergens, Der letzte Glazial/Interglazial-Zyklus, thesis, 95 pp., Justus-Liebig-Univ., Gießen, Germany, 1994.

Knies, J., Spätquatäre Paläoumweltbedingungen am nördlichen Kontinentalrand der Barents- und Kara-See: Eine Multi-Parameter-Analyse, *Ber. Polarforsch.*, *304*, 159 pp., Alfred Wegener Inst., Bremerhaven, Germany, 1999.

Knies, J., and R. Stein, New aspects of organic carbon deposition and its paleoceanographic implications along the northern Barents Sea margin during the last 30,000 years, *Paloceanography*, *13*, 384–394, 1998.

Knies, J., C. Vogt, and R. Stein, Late Quaternary growth and decay of the Svalbard/Barents Sea ice sheet and paleoceanographic evolution in the adjacent Arctic Ocean, *Geo Mar. Lett.*, *18*(3), 195–202, 1999.

Knies, J., N. Nowaczyk, C. Müller, C. Vogt, and R. Stein, A multiproxy approach to reconstruct the environmental changes along the Eurasian continental margin over the last 150,000 years, *Mar. Geol.*, *163*, 317–344, 2000.

Knies, J., H. P. Kleiber, J. Matthiessen, C. Müller, and N. Nowaczyk, Marine records indicate maximum extent of Saalian and Weichselian ice-sheets along the northern Eurasian margin, *Quat. Sci. Rev.*, *31*, 45–64, 2001.

Kohfeld, K., R. Fairbanks, S. L. Smith, and I. D. Walsh, *Neogloboquadrina pachyderma* (sinistral coiling) as paleoceanographic tracers in polar oceans: Evidence from northeast water Polynya plankton tows, sediment traps, and surface sediments, *Paleoceanography*, *11*(6), 679–700, 1996.

Köhler, S. E. I., Spätquatäre paläo-ozeanographische Entwicklung des Nordpolarmeeres und Europäischen Nordmeeres anhand von Sauerstoff- und Kohlenstoffisotopenverhältnissen der planktischen Foraminifere *Neogloboquadrina pachyderma* (sin.), *GEOMAR Rep. 13*, 104 pp., Geomar Res. Cent. for Mar. Geosci., Kiel, Germany, 1992.

Kuijpers, A. H., S. R. Troelstra, M. Wisse, S. H. Nielsen, and T. C. E. van-Weering, Norwegian Sea overflow variability and NE Atlantic surface hydrography during the past 150,000 years, *Mar. Geol.*, *152*, 101–127, 1998.

Kutzbach, J. E., and P. J. Guetter, The influence of changing orbital parameters and surface boundary conditions on climate simulations for the past 18,000 years, *J. Atmos. Sci.*, *43*(16), 1726–1759, 1986.

Landvik, J. Y., S. Bondevik, A. Elverhøi, W. Fjeldskaar, J. Mangerud, M. J. Siegert, J. I. Svendsen, and T. O. Vorren, The Last Glacial Maximum of Svalbard and the Barents Sea area: Ice sheet extent and configuration, *Quat. Sci. Rev.*, *17*, 43–75, 1998.

Lassen, S., E. Jansen, K. L. Knudsen, A. Kuijpers, M. Kristensen, and K. Christensen, Northeast Atlantic sea surface circulation during the past 30–10 ^{14}C kyr B.P., *Paleoceanography*, *14*(5), 616–625, 1999.

Mangerud, J., V. Astakhov, and J.-I. Svendsen, The extent of the Barents-Kara ice sheet during the Last Glacial Maximum, *Quat. Sci. Rev.*, *21*, 111–119, 2002.

Markussen, B., Late Quarternary sedimentation and paleoceanography in the eastern Arctic

Ocean, M. S. thesis, 174 pp., Dept. of Geol., Univ. of Oslo, Oslo, 1986.

Markussen, B., R. Zahn, and J. Thiede, Late Quaternary sedimentation in the eastern Arctic basin: Stratigraphy and depositional environment, *Palaeogeogr. Palaeoclimatol. Palaeoecol.*, *50*, 271–284, 1985.

Mix, A., E. Bard, and R. Schneider, Environmental processes of the ice age: Land, oceans, glaciers (EPILOG), *Quat. Sci. Rev.*, *20*, 627–657, 2001.

Morison, J., K. Aagaard, and M. Steele, Report on Study of the Arctic Change Workshop held November 10–12, 1997, University of Washington, Seattle, Washington, *Rep. 8*, Arctic Sys. Sci., Seattle, Wash., 1998.

Nørgaard-Pedersen, N., Late Quaternary Arctic Ocean sediment records: Surface ocean conditions and provenance of ice-rafted debris, *GEOMAR Rep. 65*, 115 pp., Geomar Res. Cent. for Mar. Geosci., Kiel, Germany, 1997.

Nørgaard-Pedersen, N., R. F. Spielhagen, J. Thiede, and H. Kassens, Central Arctic surface ocean environment during the past 80,000 years, *Paleoceanography*, *13*(2), 193–204, 1998.

Notholt, H., The implication of the "North East Water"—Polynya on the sedimentation by NE-Greenland and late Quaternary paleo-oceanic investigations, *Ber. Polarforsch.*, *275*, 182 pp., 1998.

Nürnberg, D., I. Wollenburg, D. Dethleff, H. Eicken, H. Kassens, T. Letzig, E. Reimnitz, and J. Thiede, Sediments in Arctic sea ice: Implications for entrainment, transport, and release, *Mar. Geol.*, *119*, 185–214, 1994.

Pagels, U., Sedimentologische Untersuchungen und Bestimmung der Karbonatlösung in spätquartären Sedimenten des östlichen arktischen Ozeans, *GEOMAR Rep. 10*, 106 pp., Geomar Res. Cent. for Mar. Geosci., Kiel, Germany, 1991.

Pflaumann, U., et al., The Glacial North Atlantic: Sea-surface conditions reconstructed by GLAMAP 2000, *Paleoceanography*, *18*, doi:10.1029/2002PA000774, in press, 2003.

Phillips, R. L., and A. Grantz, Quaternary history of sea ice and paleoclimate in the Amarasia basin, Arctic Ocean, as recorded in the cyclical strata of Northwind Ridge, *Geol. Soc. Am. Bull.*, *109*(9), 1101–1115, 1997.

Poore, R. Z., L. Osterman, W. B. Curry, and R. L. Phillips, Late Pleistocene and Holocene meltwater events in the western Arctic Ocean, *Geology*, *27*(8), 759–762, 1999.

Rosell-Melé, A., and P. Comes, Evidence for a warm Last Glacial Maximum in the Nordic Seas or an example of shortcomings in $U^{k'}_{37}$ and U^{k}_{37} to estimate low sea surface temperature?, *Paleoceanography*, *14*(6), 770–776, 1999.

Rosell-Melé, A., and N. Koç, Paleoclimatic significance of the stratigraphic occurrence of photosynthetic biomarker pigments in the Nordic Seas, *Geology*, *25*, 49–52, 1997.

Rothrock, D. A., Y. Yu, and G. A. Maykut, Thinning of the Arctic sea-ice cover, *Geophys. Res. Lett.*, *26*(23), 3469–3472, 1999.

Rudels, B., E. P. Jones, L. G. Anderson, and G. Kattner, On the intermediate depth waters of the Arctic Ocean, in *The Polar Oceans and Their Role in Shaping the Global Environment*, *Geophys. Monogr. Ser.*, vol. 85, edited by O. M. Johannesen, R. D. Muench, and J. E. Overland, pp. 33–46, AGU, Washington, D. C., 1994.

Sarnthein, M., et al., Variations in Atlantic surface ocean paleoceanography, 50°–80°N: A time-slice record of the last 30,000 years, *Paleoceanography*, *10*(6), 1063–1094, 1995.

Sarnthein, M., R. Gersonde, S. Niebler, U. Pflaumann, R. Spielhagen, J. Thiede, G. Wefer, and W. Weinelt, Overview of Glacial Atlantic Ocean Mapping (GLAMAP 2000), *Paleoceanography*, *18*(2), 1030, doi:10.1029/2002PA000769, 2003a.

Sarnthein, M., U. Pflaumann, and M. Weinelt, Past extent of sea ice in the northern North Atlantic inferred from foraminiferal paleotemperature estimates, *Paleoceanography*, *18*(2), 1047, doi:10.1029/2002PA000771, 2003b.

Schlosser, P., D. Bauch, G. Bönisch, and R. F. Fairbanks, Arctic river-runoff: Mean residence time on the shelves and in the halocline, *Deep Sea Res., Part I*, *41*(7), 1053–1068, 1994.

Seidov, D., and B. J. Haupt, Simulated ocean circulation and sediment transport in the North Atlantic during the Last Glacial Maximum and today, *Paleoceanography*, *12*, 281–306, 1997.

Sher, A., Is there any real evidence for a huge shelf ice sheet in east Siberia?, *Quat. Int.*, *28*, 39–40, 1995.

Spielhagen, R. F., Die Eisdrift in der Framstrasse während der letzten 200.000 Jahre, *GEOMAR Rep. 4*, 133 pp., Geomar Res. Cent. for Mar. Geosci., Kiel, Germany, 1991.

Spielhagen, R. F., and H. Erlenkeuser, Stable oxygen and carbon iostopes in planktic foraminifers from Arctic Ocean surface sediments: Reflection of the low salinity surface water layer, *Mar. Geol.*, *119*, 227–250, 1994.

Stein, R., C. Schubert, C. Vogt, and D. Fütterer, Stable isotope stratigraphy, sedimentation rates and paleosalinity in the latest Pleistocene to Holocene Central Arctic Ocean, *Mar. Geol.*, *119*, 333–355, 1994.

Stuiver, M., and P. J. Reimer, Extended ^{14}C database and revised CALIB radiocarbon calibration program, *Radiocarbon*, *35*, 215–230, 1993.

Stuiver, M., P. J. Reimer, E. Bard, J. W. Beck, G. S. Burr, K. A. Hughen, B. Kromer, F. G. McCormac, J. V. D. Plicht, and M. Spurk, INTCAL98 Radiocarbon Age Calibration, 24,000-0 cal BP, *Radiocarbon*, *40*(3), 1041–1083, 1998.

Svendsen, J. I., et al., Maximum extent of the Eurasian ice sheets in the Barents and Kara Sea region during the Weichselian, *Boreas*, *28*(1), 234–242, 1999.

Tarasov, P. E., O. Peyron, J. Guiot, S. Brewer, V. S. Volkova, L. G. Bezusko, N. I. Dorfeyuk, E. V. Kvavadze, I. M. Osipova, and N. K. Panova, Last Glacial Maximum climate of the former Soviet Union and Mongolia reconstructed from pollen and plant microfossil data, *Clim. Dyn.*, *15*, 227–240, 1999.

Velichko, A. A., The Pleistocene termination in northern Eurasia, *Quat. Int.*, *28*, 105–111, 1995.

Velichko, A. A., Y. M. Kononov, and M. Faustova, The last glaciation of Earth: Size and volume of ice sheets, *Quat. Int.*, *41/42*, 43–51, 1997.

Veum, T., E. Jansen, M. Arnold, I. Beyer, and J.-C. Duplessy, Water mass change in the North Atlantic and the Norwegian Sea during the past 28,000 years, *Nature*, *356*, 783–785, 1992.

Vinje, T. E., Sea ice conditions in the European sector of the marginal seas of the Arctic, 1966–75, *Nor. Polarinst. Årbok*, *1975*, 163–174, 1977.

Vinje, T. E., Sea ice distribution 1971–1980, *Nor. Polarinst. Skr.*, *179D*, 12–20, 1985.

Voelker, A. H. L., M. Sarnthein, P. M. Grootes, H. Erlenkeuser, C. Laj, A. Mazaud, M.-J. Nadeau, and M. Schleicher, Correlation of marine ^{14}C ages from the Nordic Seas with the GISP2 isotope record: Implications for ^{14}C calibration beyond 25 ka BP, *Radiocarbon*, *40*(1), 517–534, 1998.

Vogt, C., Zur Paläoozeanographie und Paläoklima im spätquartären Arktischen Ozean: Zusammensetzung und Flux terrigener und biogener Sedimentkomponenten auf dem Morris Jesup Rise und dem Yermak Plateau, *Ber. Polarforsch.*, *251*, 309 pp., Alfred Wegener Inst., Bremerhaven, Germany, 1997.

Vogt, C., J. Knies, R. F. Spielhagen, and R. Stein, Detailed mineralogical evidence for two nearly identical glacial/deglacial cycles and Atlantic water advection to the Arctic Ocean during the last 90,000 years, *Gloal. Planet. Change*, *31*, 23–44, 2001.

Volkmann, R., Planktic foraminifers in the Fram Strait and the outer Laptev Sea: Modern distribution and ecology, *J. Foraminiferal Res.*, *30*(3), 157–176, 2000.

Weinelt, M., M. Sarnthein, U. Pflaumann, H. Schulz, S. Jung, and H. Erlenkeuser, Ice-free Nordic Seas during the Last Glacial Maximum?, Potential sites of deepwater formation, *Paleoclimatology*, *1*, 283–309, 1996.

Zahn, R., B. Markussen, and J. Thiede, Stable isotope data and depositional environments in the late Quaternary Arctic Ocean, *Nature*, *314*, 433–435, 1985.

Zreda, M., J. England, F. Phillips, D. Elmore, and P. Sharma, Unblocking of the Nares Strait by Greenland and Ellesmere ice-sheet retreat 10,000 years ago, *Nature*, *398*, 139–142, 1999.

————————————

H. Erlenkeuser and P. M. Grootes, Leibniz Laboratory for Radiometric Dating and Isotope Research, Christian-Albrechts-Universität zu Kiel, Max-Eyth-Str. 11-13, D-24118 Kiel, Germany. (herlenkeuser@leibniz.uni-kiel.de; pgrootes@leibniz.uni-kiel.de)

J. Heinemeier, AMS 14C Dating Laboratory, Institute of Physics and Astronomy, University of Aarhus, DK-8000 Aarhus C, Denmark. (jh@phys.au.dk)

J. Knies, Geological Survey of Norway, Leiv Eirikssons vei 39, N-7491 Trondheim, Norway. (Jochen.Knies@NGU.NO)

N. Nørgaard-Pedersen and R. F. Spielhagen, Research Center for Marine Geosciences, GEOMAR, Kiel University, D-24148 Kiel, Germany. (nnoergaa@geomar.de)